Table IV Multiple additional mutations detected in subclones of the *IL2RG* gene

	Subclones	Mutations
Wild type	TT CCTCT T CCT T CCAACC	Wild type
Inherited mutation	TT CCTCT T CCT T CCAGCC	c.284-15A>G
No.1	TT CCTCT T CCT T CCATCC	c.284-15A>T
No.2	TT CCTCT T CCT T CCACCC	c.284-15A>C
No.3	TT CCTCT T CAT T CCAGCC	c.284-15A>G, c.284-21C>A
No.4	TT AGAGTGG CCTCT T CCT T CCAGCC	c.284-15A>G, c.284-29_284-28insAGAGTGG
No.5	TT CCTC CACCCGCCAAC	c.284-24_284-14del11ins CACCCGCCAA
No.6	TT CCTCT CAGCC	c.284-23_284-18delTCCTTC

reversions found in the patient's T cells must have occurred before or around the CD4ISP stage. Differences were observed in reversion genotypes between the TCRαβ+ cells and TCRγδ+ cells. TCRγδ+ cells had only one of the second-site reversions found in TCRαβ+ cells in addition to a true-back reversion (No.3 in Table V). The identification of fewer reversions in the patient's TCRγδ+ compared to TCRαβ+ cells may reflect the greater abundance of TCRαβ+ cells, increasing the likelihood of the stochastic occurrence of additional reversions [18]. Although no reversions in the patient's B cells or monocytes were observed, it is possible that the reversions occurred in the progenitor at the stage before commitment to T cells and may reflect the unique nature of T cell proliferation and expansion [19].

Reversion mosaicism has previously been reported in SCID-X1 patients with *IL2RG* mutations, but it was accompanied by reduced T cell number and low proliferative response to mitogens [2, 3]. The paradoxical nature of the patient's cellular immunity, a history of uneventful varicella infection, and the occurrence of widespread warts with very few naïve T cells prompted an evaluation of his T cell function. The TCR Vβ repertoire analysis of CD4+ and CD8+ T cells revealed comparable diversity to the normal controls (data not shown). CDR3 spectratyping analysis revealed the patient CD4+ T cells had as much variety as the normal controls, but his CD8+ T cells displayed restricted diversity (Fig. 3a). To evaluate the antigen-specific response of the patient's T cells, response to VZV was measured. The DTH reaction to subcutaneous VZV antigen and the IFN-γ production from VZV antigen-stimulated PBMCs measured by an ELISPOT assay were comparable to those of normal controls (Table I and Fig. 3b). These data suggested that the patient maintained normal cellular immune responses *in vivo* as well as having normal *in vitro* IFN-γ production ability against VZV antigen. Multiple reversions from intronic mutations could provide a sufficient number of normally functioning T cells and may improve the clinical phenotype compared to previously reported cases with single reversions. However, the number of TRECs in the patient's PBMCs (<10 copies/μg DNA) suggested a low level of recent thymic output, and the restricted diversity of TCRs observed in the patient's CD8+ cells might reflect the exhaustion of the T cell reservoir. To gain further insight, the long-term immunologic status of the patient was evaluated prospectively for 5 years. Absolute counts of CD4+ and CD8+ T cells as well as mitogen-induced T cell proliferation responses were measured every 2–5 months (Fig. 4). Unexpectedly, the number of both CD4+ and CD8+ T cells and mitogen-induced T cell proliferation responses were stable and the patient remained healthy over this period. In recent years, the effector memory subset of CD8+ T cells (CD8+/CD45RA+/CCR7-) has been taken as a marker of cell exhaustion or replicative senescence [20]. However, the majority of CD8+ T cells of the patient were memory CD8+ T cells (CD8+/CD45RA-/CCR7±) and the population of effector memory CD8+ T cells was very small (Table II). These data

Table V Clonal analysis of somatic mosaicism of the *IL2RG* gene in various cell lineages

	Wild type	Inherited mutation	No.1	No.2	No.3	No.4	No.5	No.6
TCRαβ+	21 % (7/33)	12 % (4/33)	9 % (3/33)	12 % (4/33)	21 % (7/33)	9 % (3/33)	6 % (2/33)	9 % (3/33)
TCRγδ+	2 % (1/42)	2 % (1/42)	0 % (0/42)	0 % (0/42)	95 % (40/42)	0 % (0/42)	0 % (0/42)	0 % (0/42)
CD3+	5 % (2/39)	5 % (2/39)	26 % (10/39)	13 % (5/39)	38 % (15/39)	3 % (1/39)	10 % (4/39)	0 % (0/39)
CD4+	32 % (25/79)	3 % (2/79)	13 % (10/79)	19 % (15/79)	16 % (13/79)	3 % (2/79)	3 % (2/79)	13 % (10/79)
CD8+	10 % (7/73)	4 % (3/73)	21 % (15/73)	19 % (14/73)	25 % (18/73)	8 % (6/73)	12 % (9/73)	1 % (1/73)
CD14+	0 % (0/33)	100 % (33/33)	0 % (0/33)	0 % (0/33)	0 % (0/33)	0 % (0/33)	0 % (0/33)	0 % (0/33)
CD19+	0 % (0/30)	100 % (30/30)	0 % (0/30)	0 % (0/30)	0 % (0/30)	0 % (0/30)	0 % (0/30)	0 % (0/30)

Data represent the percentages of each additional mutant subclone in each lineage. The ratio indicates the number of each mutant clone in various cell lineages as compared to the total number of clones analyzed, based on subcloning and sequencing analysis

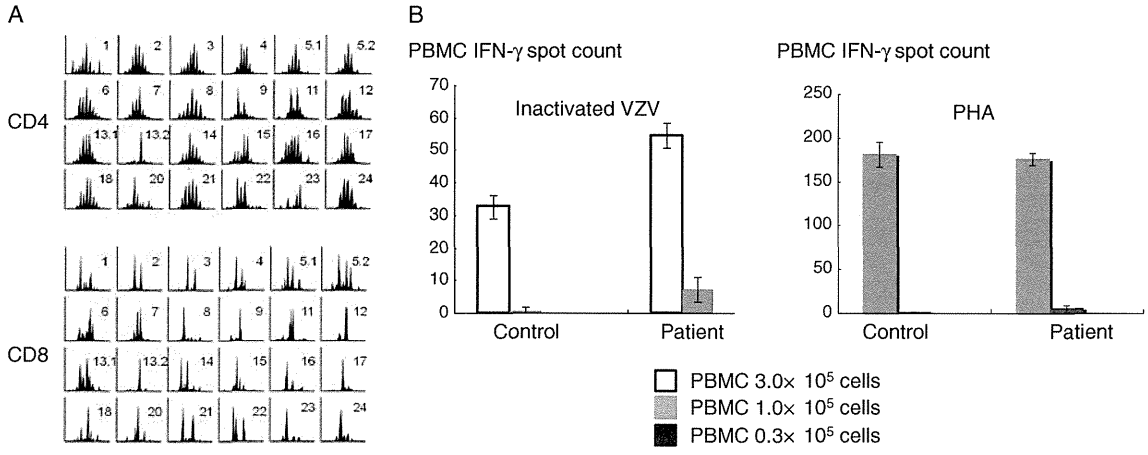

Fig. 3 Functional evaluation of T cells at 9 years old. **a** CDR3 spectratyping of the TCRVβ chain. Each TCRVβ fragment was amplified from cDNA with one of 24Vβ-specific primers (each Vβ chain is indicated). The size distribution of the PCR products was determined by an automated sequencer and GeneScan software. The CDR3 size distribution in CD4+ and CD8+ T cells from the patient is shown. **b** Elispot analysis of IFN-γ production as a measure of T cell function. (LEFT) Varicella-specific immune response to varicella zoster (VZV) antigen *in vitro*. Patient and control (from a healthy with a previous history of varicella infection) PBMCs ($0.3\text{-}3\times10^5$) were stimulated with inactivated VZV antigen or (RIGHT) PHA. Data are shown as mean ± SD

demonstrated that the patient maintained a certain level of T cell immunity for over a decade, despite the fact that the supply of fresh T cells from the thymus was limited and the patient suffered from generalized warts. Further follow up is required to determine if the patient can continue to maintain long-term T cell immunity.

In conclusion, this study indicates that it is critical to determine the NK cell number to avoid overlooking reversion mosaicism of SCID-X1. In addition, it has been shown that a number of *IL2RG* gene reversions can restore T cell functions and maintain T cell immunity against viral infection for at least 14 years.

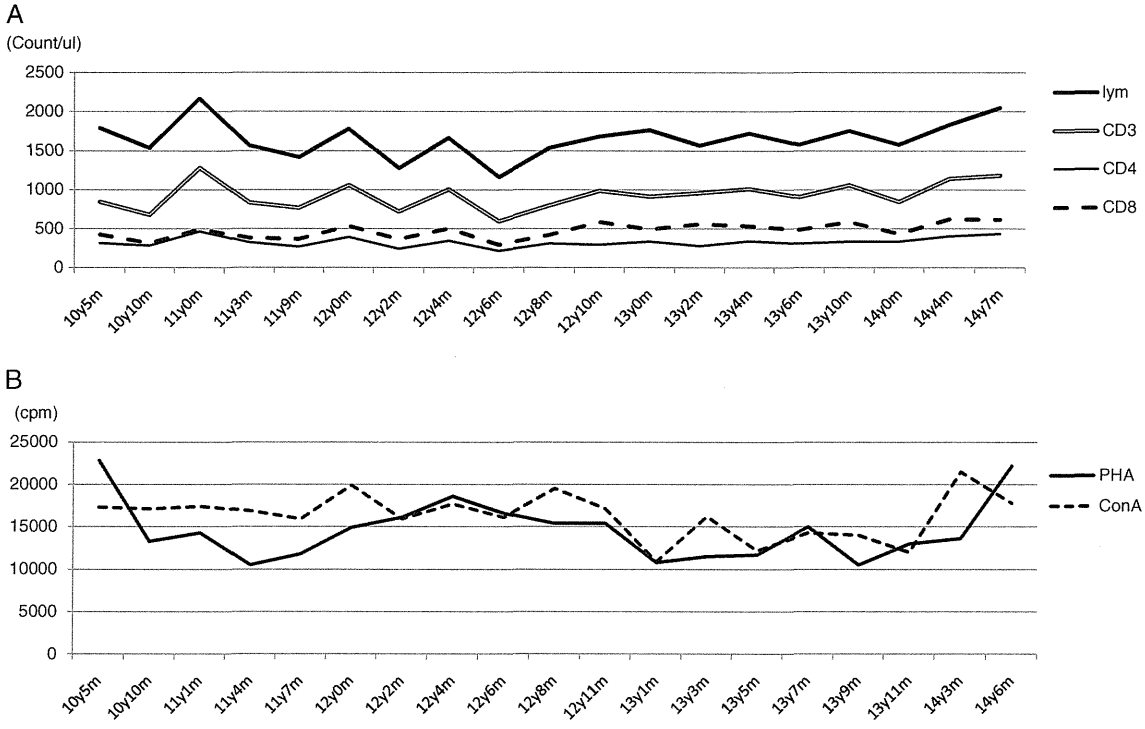

Fig. 4 Long term evaluation of T cell number and mitogen-induced proliferative response. **a** Absolute counts (per μl) of total lymphocytes (lym), CD3+ cells, CD4+ cells and CD8+ cells were measured for 4 years. **b** T cell proliferation in response to PHA (*solid line*) and Con A (*dotted line*). Healthy control values for PHA range from 20,500 to 56,800 cpm and for Con A from 20,500 to 65,700 cpm

Acknowledgements We are grateful to the patient and his family for their participation. We also thank Takeda Pharmaceutical Company (Osaka, Japan) for kindly providing recombinant IL-2.

Authors' contributions T.K. performed experiments and wrote the paper. M.S. and Ka.I. performed experiments. R.N. designed the research, wrote the paper and analyzed data. Y.T. wrote the paper and analyzed data. T.M. treated the patient and analyzed data. S.O., Y.M., N.N., Ko.I, S.N., T.W. and A.Y. performed experiments and discussed the research. T.H. and T.N. designed the research.

Conflict of Interests The authors declare no competing financial interests.

References

1. Buckley RH. Primary immunodeficiency diseases: dissectors of the immune system. Immunol Rev. 2002;185:206–19.
2. Stephan V, Wahn V, Le Deist F, Dirksen U, Broker B, Muller-Fleckenstein I, et al. Atypical X-linked severe combined immunodeficiency due to possible spontaneous reversion of the genetic defect in T cells. N Engl J Med. 1996;335(21):1563–7.
3. Speckmann C, Pannicke U, Wiech E, Schwarz K, Fisch P, Friedrich W, et al. Clinical and immunologic consequences of a somatic reversion in a patient with X-linked severe combined immunodeficiency. Blood. 2008;112(10):4090–7.
4. Hirschhorn R, Yang DR, Puck JM, Huie ML, Jiang CK, Kurlandsky LE. Spontaneous in vivo reversion to normal of an inherited mutation in a patient with adenosine deaminase deficiency. Nat Genet. 1996;13(3):290–5.
5. Hirschhorn R. In vivo reversion to normal of inherited mutations in humans. J Med Genet. 2003;40(10):721–8.
6. Ariga T, Kondoh T, Yamaguchi K, Yamada M, Sasaki S, Nelson DL, et al. Spontaneous in vivo reversion of an inherited mutation in the Wiskott-Aldrich syndrome. J Immunol. 2001;166(8):5245–9.
7. Wada T, Toma T, Okamoto H, Kasahara Y, Koizumi S, Agematsu K, et al. Oligoclonal expansion of T lymphocytes with multiple second-site mutations leads to Omenn syndrome in a patient with RAG1-deficient severe combined immunodeficiency. Blood. 2005;106(6):2099–101.
8. Nishikomori R, Akutagawa H, Maruyama K, Nakata-Hizume M, Ohmori K, Mizuno K, et al. X-linked ectodermal dysplasia and immunodeficiency caused by reversion mosaicism of NEMO reveals a critical role for NEMO in human T-cell development and/or survival. Blood. 2004;103(12):4565–72.
9. Uzel G, Tng E, Rosenzweig SD, Hsu AP, Shaw JM, Horwitz ME, et al. Reversion mutations in patients with leukocyte adhesion deficiency type-1 (LAD-1). Blood. 2008;111(1):209–18.
10. Ariga T, Oda N, Yamaguchi K, Kawamura N, Kikuta H, Taniuchi S, et al. T-cell lines from 2 patients with adenosine deaminase (ADA) deficiency showed the restoration of ADA activity resulted from the reversion of an inherited mutation. Blood. 2001;97(9):2896–9.
11. Konno A, Okada K, Mizuno K, Nishida M, Nagaoki S, Toma T, et al. CD8alpha alpha memory effector T cells descend directly from clonally expanded CD8alpha+ beta high TCRalpha beta T cells in vivo. Blood. 2002;100(12):4090–7.
12. Sadaoka K, Okamoto S, Gomi Y, Tanimoto T, Ishikawa T, Yoshikawa T, et al. Measurement of varicella-zoster virus (VZV)-specific cell-mediated immunity: comparison between VZV skin test and interferon-gamma enzyme-linked immunospot assay. J Infect Dis. 2008;198(9):1327–33.
13. Kamiya H, Ihara T, Hattori A, Iwasa T, Sakurai M, Izawa T, et al. Diagnostic skin test reactions with varicella virus antigen and clinical application of the test. J Infect Dis. 1977;136(6):784–8.
14. Morinishi Y, Imai K, Nakagawa N, Sato H, Horiuchi K, Ohtsuka Y, et al. Identification of severe combined immunodeficiency by T-cell receptor excision circles quantification using neonatal guthrie cards. J Pediatr. 2009;155(6):829–33.
15. Tassara C, Pepper AE, Puck JM. Intronic point mutation in the IL2RG gene causing X-linked severe combined immunodeficiency. Hum Mol Genet. 1995;4(9):1693–5.
16. Reese MG, Eeckman FH, Kulp D, Haussler D. Improved splice site detection in Genie. J Comput Biol. 1997;4(3):311–23.
17. Sleasman JW, Harville TO, White GB, George JF, Barrett DJ, Goodenow MM. Arrested rearrangement of TCR V beta genes in thymocytes from children with X-linked severe combined immunodeficiency disease. J Immunol. 1994;153(1):442–8.
18. Joachims ML, Chain JL, Hooker SW, Knott-Craig CJ, Thompson LF. Human alpha beta and gamma delta thymocyte development: TCR gene rearrangements, intracellular TCR beta expression, and gamma delta developmental potential–differences between men and mice. J Immunol. 2006;176(3):1543–52.
19. Freitas AA, Rocha B. Population biology of lymphocytes: the flight for survival. Annu Rev Immunol. 2000;18:83–111.
20. Appay V, van Lier RA, Sallusto F, Roederer M. Phenotype and function of human T lymphocyte subsets: consensus and issues. Cytometry A. 2008;73(11):975–83.

clinical nephrology
Original

ISSN 0301-0430

DOI 10.5414/CN107344
e-pub: December 21, 2011

Evaluation of T-Cell receptor diversity in pediatric patients with minimal change nephrotic syndrome

Kazuhide Ohta[1,2], Masaki Shimizu[2], Tadafumi Yokoyama[1,2], Sayaka Nishio[2], Kazuyuki Ueno[2], Akiko Seno[2] and Akihiro Yachie[2]

[1]Department of Pediatrics, Kanazawa Medical Center, National Hospital Organization, Kanazawa and [2]Department of Pediatrics, School of Medicine, Institute of Medical, Pharmaceutical, and Health Sciences, Kanazawa University, Kanazawa, Japan

Key words
T-cell receptor (TCR) – Vβ repertoire – CDR3 size – distribution – minimal change nephrotic syndrome (MCNS)

Abstract. Aims: To further elucidate the clinical relevance of T-cell abnormalities in minimal change nephrotic syndrome (MCNS), and to predict the consequences of MCNS, we studied T-cell receptor (TCR) diversity by analyzing CDR3 size distribution and the frequency of Vβ repertoire usage. Methods: Participants comprised 36 pediatric patients with MCNS. 18 were frequent relapsers (FRs) and/or steroid-dependent (SD) and 18 were non-frequent relapsers (NFRs). Serial changes in TCR Vβ repertoires were analyzed for these two groups of patients. Frequencies of Vβ repertoire usage were determined by flow cytometry, and TCR CDR3 length distribution was analyzed by GeneScan. Results: In NFRs, abnormalities in the distribution of Vβ repertoires were few in both $CD4^+$ and $CD8^+$ T cells. In FRs/SD patients, patterns were normal in $CD4^+$ T cells, while selected Vβ repertoires were significantly increased in $CD8^+$ T cells in some patients. Furthermore, TCR diversity was significantly reduced in $CD8^+$ T cells in FRs/SD patients, as shown by marked skewing of CDR3 size distributions. Of note was the finding that some FRs/SD patients showed improvements in the initially abnormal TCR diversity with improvement in clinical symptoms, eventually becoming NFRs. Conclusion: Analysis of TCR diversity may delineate the subgroup of FRs/SD patients and provide a rationale for early intervention with immunosuppressive therapy for these patients.

Received
June 10, 2011;
accepted in revised form
September 5, 2011

Correspondence to
K. Ohta, MD, PhD
Department of Pediatrics, Kanazawa Medical Center, National Hospital Organization, 1-1 Shimo-Ishibikimachi, Kanazawa, Ishikawa 920-8650, Japan
kohta@kinbyou.hosp.go.jp

Introduction

Minimal change nephrotic syndrome (MCNS) in childhood is characterized by heavy proteinuria and generalized edema. Therapy for MCNS has been well established through numerous clinical studies and mainly consists of oral steroids [1, 2]. In cases of frequently relapsing and/or steroid-dependent MCNS, additional immunosuppressive drugs such as cyclophosphamide or cyclosporine have been approved. Better treatment could be provided if such patients could be differentiated from non-frequent relapsers (NFRs) at disease onset.

Previous studies have suggested that T cells play a major role in the pathogenesis of MCNS [3, 4, 5]. Some evidence suggests that this syndrome may represent a primary T-cell disorder that leads to glomerular podocyte dysfunction [6, 7]. Patients requiring prolonged steroid therapy or immunosuppressive agents might thus be anticipated to show abnormalities in T-cell function. We investigated distortions in T-cell receptor (TCR) diversity by analyzing CDR3 size distribution and Vβ gene usage frequency, to further elucidate the clinical relevance of T-cell abnormality in the pathogenesis of MCNS. We also examined whether our results could be used to predict the steroid-responsiveness of MCNS patients.

Materials and methods

Patients and controls

We enrolled 36 MCNS patients (21 males, 15 females; mean age 9.4 years; range, 1 – 21 years) from the Department of Pediatrics at Kanazawa University Hospital, or its affiliated hospitals, between 2000 and 2009. 20 healthy adults were enrolled as normal controls for analysis of the Vβ repertoire, and 6 healthy children (age range 0 – 11 years) were enrolled as con-

trols for the analysis of CDR3 size distributions. Approval for this study was obtained from the Human Research Committee of Kanazawa University Graduate School of Medical Science, and informed consent to participate in this study was obtained from each patient and/or their parents according to the Declaration of Helsinki. MCNS patients were classified clinically as follows. NFRs (n = 18) responded to steroids and the frequency of relapse was less than twice during the first 6 months. Frequent relapsers (FRs) (n = 13) were defined as showing an initial response to steroids, with a subsequent steroid-free period > 2 weeks, followed by ≥ 2 relapses within 6 months. Steroid-dependent (SD) patients (n = 5) were defined as showing initial steroid-induced remission with relapses during tapering of corticosteroids, or ≤ 2 weeks after steroid withdrawal. Relapse was diagnosed when proteinuria of more than 2+ (by dipstick) or 100 mg/dl continued for 3 consecutive days.

Cell preparation

Peripheral blood mononuclear cells (PBMCs) from patients and normal controls were isolated from heparinized venous blood samples by density gradient centrifugation over Ficoll (Histopaque; Sigma, St. Louis, MO, USA) and T-cells were separated using the E rosette method [8, 9]. Subsequently, T cells and their subsets (CD4, CD8) were selected using Dynabeads M-450 CD4, CD8 (Dynal AS, Oslo, Norway) [8, 9].

RNA extraction and cDNA synthesis

Total cellular RNA was isolated using TRIZOL reagent in accordance with the instructions from the manufacturer (Gibco BRL, Bethesda, MD, USA), and first-strand cDNA was generated from 2 μg of total RNA with random hexamers and RAV-2 reverse transcriptase (TaKaRa Bio, Shiga, Tokyo, Japan). The concentration of RNA was measured using a GeneQuant pro RNA/DNA Calculator (Amersham Pharmacia Biotech, Cambridge, UK) [10].

Determination of Vβ repertoires

TCR Vβ repertoire distribution was analyzed using 3-color flow cytometry. After red blood cell (RBC) lysis and washing in phosphate-buffered saline (PBS), samples were incubated with appropriate phycoerythrin (PE)-conjugated monoclonal antibodies with specificity for TCR Vβ (Coulter Immunotech, Marseille, France) for 30 min on ice, followed by fluorescein isothiocyanate (FITC)-conjugated anti-CD8 antibody (Becton, Dickinson and Co., San Diego, CA, USA) and R-PE-Cy5 (PC5)-conjugated anti-CD4 antibody (DAKO, Glostrup, Denmark) for 15 min. After washing in PBS, 3-color analysis was performed with the FACSCalibur instrument (Becton Dickinson Biosciences, Franklin Lakes, NJ, USA). We analyzed the TCR Vβ repertoire distribution in normal controls (n = 20) (Figure 1A) and calculated means ± standard deviation.

Determination of CDR3 size distribution

CDR3 spectratyping was performed as previously described [8, 9]. Briefly, cDNA was polymerase chain reaction (PCR)-amplified through 35 cycles (94 °C for 1 min, 55 °C for 1 min, and 72 °C for 1 min) with a primer specific for 24 different Vβ subfamilies (Vβs 1 – 20 [11] and Vβs 21 – 24 [12]) and a fluorescent BC primer (Figure 2A) [11]. Fluorescent PCR products were mixed with formamide and a size standard (GeneScan-500 TAMRA; Applied Biosystems, Foster City, CA, USA). After denaturation for 2 min at 90 °C, products were analyzed using an automated 310 DNA sequencer (Applied Biosystems) and the data were analyzed with GeneScan software (Applied Biosystems). Overall complexity within a Vβ subfamily was determined by counting the number of discrete peaks and determining their relative sizes on the spectratype histogram, as described elsewhere [13]. Variety in a Vβ repertoire appears as multiple peaks (Gaussian distribution) (Figure 2B), while a repertoire lacking variety shows few peaks (skewed distribution) (Figure 2C). CDR3 size spectratyping of Vβ subfamilies in normal controls is shown in Figure 1B.

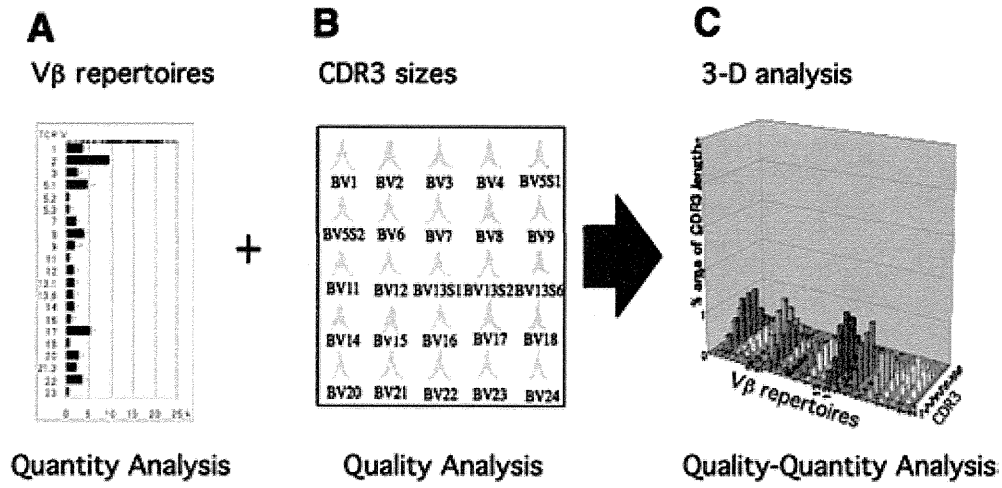

Figure 1. Vβ repertoires, CDR3 sizes, and 3-dimensional analysis of TCR diversity in normal controls. These figures show normal patterns of quantitative analysis, qualitative analysis, and a combination of both.

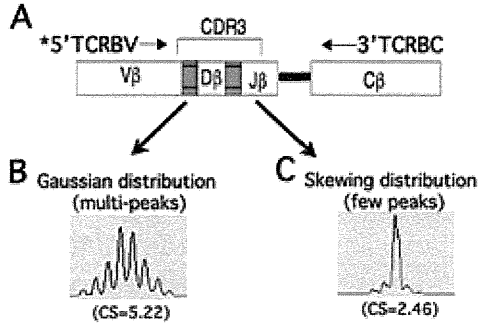

Figure 2. Spectratyping of CDR3 size. Primer for 24 different Vβ subfamilies and a fluorescent BC primer (A). Variety in a Vβ repertoire results in multiple peaks, representing a Gaussian distribution (B). A repertoire lacking variety shows few peaks, representing a skewed distribution (C).

We used a complexity scoring system [13] to facilitate interpretation: complexity score (CS) = (sum of all peak heights/sum of major peak heights) × (number of major peaks). Major peaks were defined as those with amplitude ≥ 10% of the sum of all peak heights on the spectratype histogram. CDR3 size analysis revealed multiple peaks with a Gaussian distribution in normal controls.

Three-dimensional graphic display of TCR diversity through a combination of CDR3 size analysis and Vβ repertoire distribution

Qualitative alterations in TCR Vβ repertoires obtained by CDR3 spectratyping were combined with quantitative analyses of specific $V\beta^+$ $CD4^+$ and $CD8^+$ T cells for each Vβ subfamily and plotted as landscape columns, as previously described [14, 15, 16].

Statistical analysis

The Mann-Whitney U-test was used for analysis of unpaired samples. Correlations were tested using the Spearman rank analysis test. Values of $p < 0.05$ were considered statistically significant.

Results

Distribution of Vβ repertoires in different groups of MCNS patients

We analyzed Vβ repertoire distributions in MCNS patients and the 20 normal controls. Representative profiles from each group are shown in Figure 3. Among NFRs, abnormalities in Vβ repertoire distribution were infrequent in both $CD4^+$ and $CD8^+$ T cells. In some FRs/SD patients, selected Vβ repertoires were significantly increased in $CD8^+$ T cells (asterisks), but this tendency was much less pronounced in $CD4^+$ T cells. Increased Vβ repertoires were of various types, and increases characteristic of MCNS were not found. While we were able to compare each group visually in this analysis, objective comparison of each group was difficult.

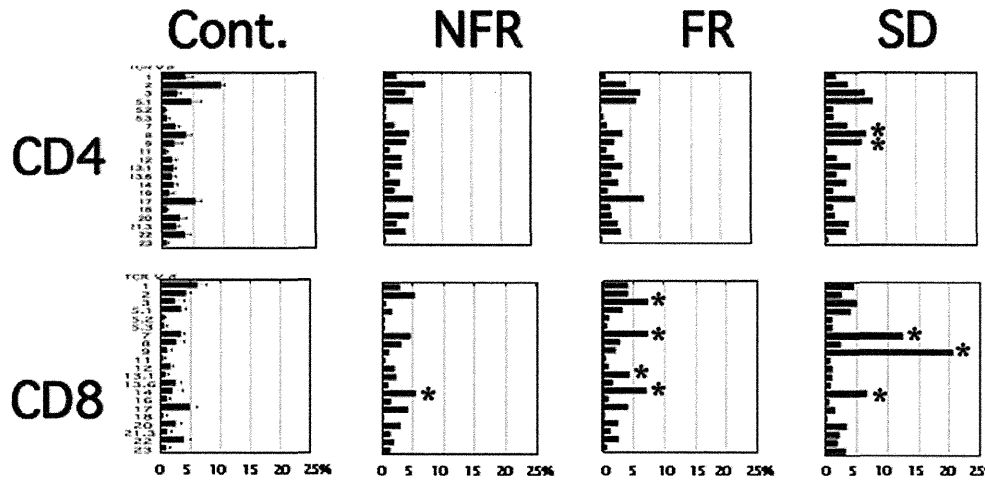

Figure 3. Vβ repertoire distribution in different groups of MCNS patients. * indicates increased Vβ repertoires above healthy controls. In some FRs/SD patients, selected Vβ repertoires were significantly increased in $CD8^+$ T cells (*), but this tendency was much less pronounced in $CD4^+$ T cells.

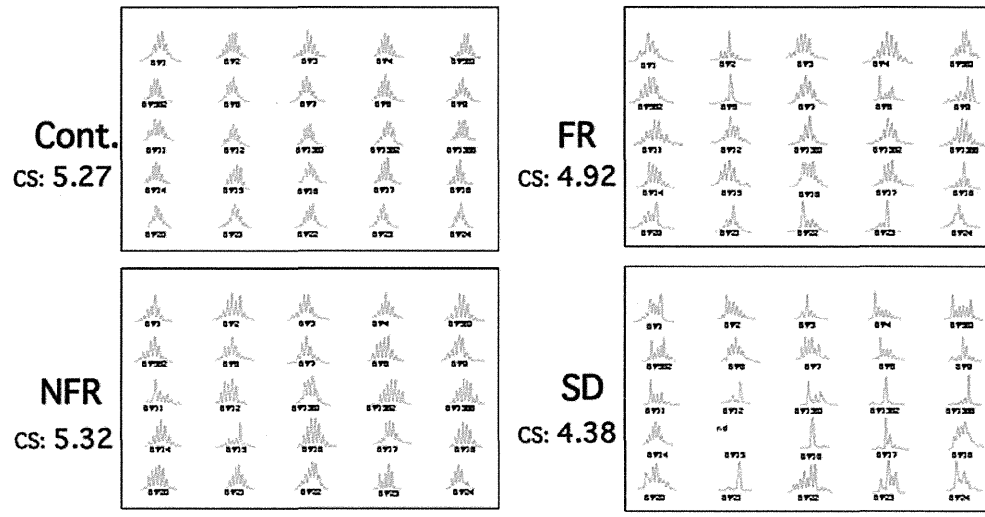

Figure 4. CDR3 size distributions on CD8+ T cells of typical cases in different groups of MCNS patients: A: normal control; B: NFR; C: FR; D: SD. In FRs/SD patients, CDR3 size distributions showed an oligoclonal or monoclonal pattern in many Vβ subfamilies of CD8+ T cells. Mean CS values for FR (4.92) and SD (4.38) patients were low in comparison with normal control (5.27) and NFR (5.32) patients. Numerical values in parentheses represent mean CS value for each group.

Distribution of CDR3 sizes in different groups of MCNS patients

Among NFRs, CDR3 size distributions of all Vβ subfamilies in $CD8^+$ T cells showed normal patterns (Gaussian distribution). Mean CS values were high in normal controls (5.27) and NFRs (5.32). In representative FRs/SD patients, CDR3 size distributions showed an oligoclonal or monoclonal pattern in many Vβ subfamilies. As a result, mean CS values were low in FR (4.92) and SD (4.38) patients (Figure 4). No such tendency was observed in $CD4^+$ T cells.

To compare CS values between $CD4^+$ T cells and $CD8^+$ T cells, CS values for each Vβ subfamily were plotted. Representative plotted profiles from each group are shown in Figure 5. In NFRs, CDR3 size distributions showed normal patterns and all CS values were within the range of 5.0 – 6.0. In contrast, CDR3 size distributions showed oligoclonal or monoclonal patterns and CS values varied greatly between individual FRs/SD patients. In particular, CS values were < 4.0 in many Vβ subfamilies among FRs/SD patients. Such findings were more apparent in $CD8^+$ T cells than in $CD4^+$ T cells.

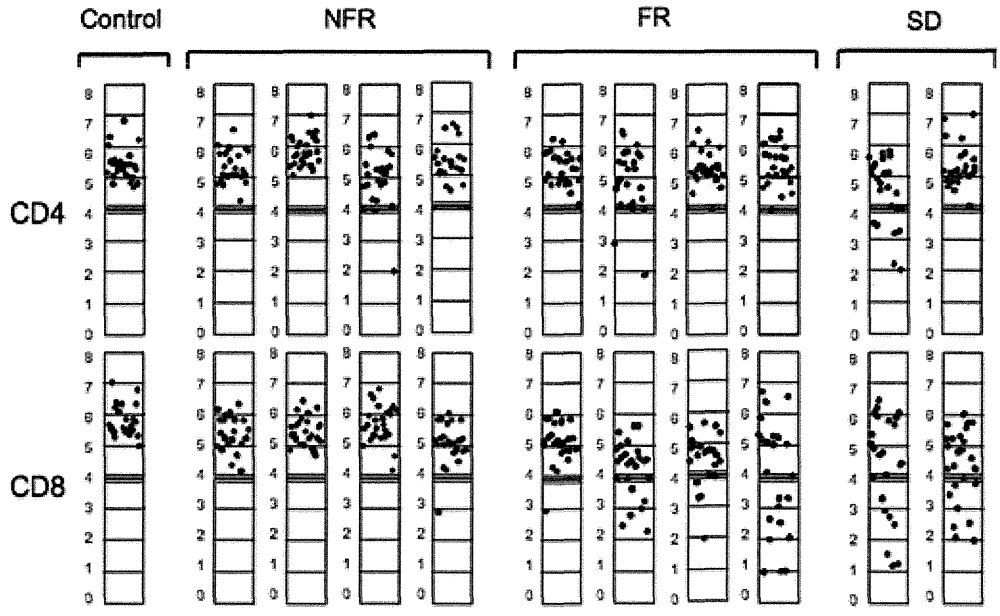

Figure 5. Distribution of CS values in representative patients from each group. Many CS values of Vβ repertoires in FRs/SD patients were < 4.0.

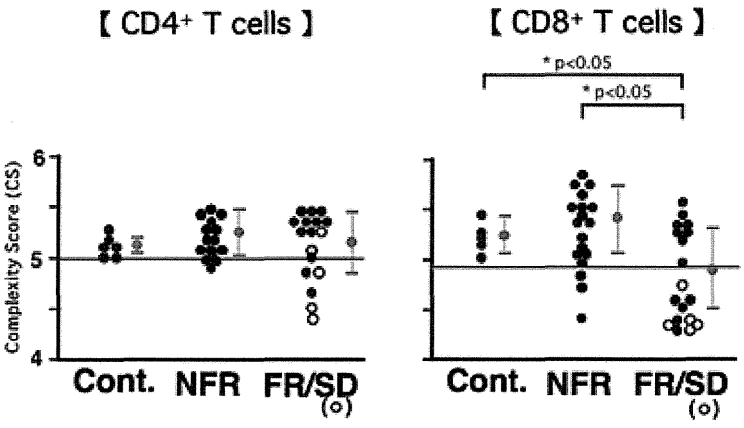

Figure 6. Mean CS values for all patients. A significant difference in mean CS values was apparent between normal controls or NFRs and FRs/SD patients. The value of -2 standard deviations is shown in a line. Control, n = 6 ($CD4^+$ T cells, n = 6; $CD8^+$ T cells, n = 5); NFR, n = 18 ($CD4^+$ T cells, n = 14; $CD8^+$ T cells, n = 18); FR, n = 13 ($CD4^+$ T cells, n = 12; $CD8^+$ T cells, n = 13); SD, n = 5 ($CD4^+$ T cells, n = 5; $CD8^+$ T cells, n = 5).

To further emphasize CS distribution characteristics, mean CS values in $CD4^+$ and $CD8^+$ T cells from all patients are presented in Figure 6. In $CD4^+$ T cells, mean CS values were 5.14 ± 0.06 in normal controls, 5.26 ± 0.21 in NFRs, and 5.13 ± 0.31 in FRs/SD patients. These differences were not statistically significant. In $CD8^+$ T cells, mean CS values were 5.25 ± 0.15 in normal controls, 5.42 ± 0.33 in NFRs, and 4.90 ± 0.44 in FRs/SD patients. The difference between mean CS values in normal controls/NFRs and FRs/SD patients was statistically significant. In the FR/SD group, mean CS values in $CD8^+$ T cells were below –2 standard deviations or < 4.95 in approximately half of all patients. In other words, a MCNS patient is expected to be FRs/SD at a sensitivity of 56% and specificity of 77%, when the mean CS value in $CD8^+$ T cells is < 4.95. Mean CS values in $CD8^+$ T cells might thus be applicable for objective prediction of the clinical course.

Effect of short-term steroid therapy on TCR diversity

We examined whether short-term steroid therapy itself could have a direct effect on TCR diversity. A representative example is shown in Figure 7. Both TCR Vβ repertoires and CDR3 size distributions in $CD8^+$ T cells showed similar patterns after 2 weeks of steroid therapy and remained stable after 8 weeks when the patient was in remission without steroids.

Improvement in TCR diversity with clinical response to therapy

Figure 8 shows results for a FR who underwent repeated analyses over the course of 3 years after disease onset. The patient was

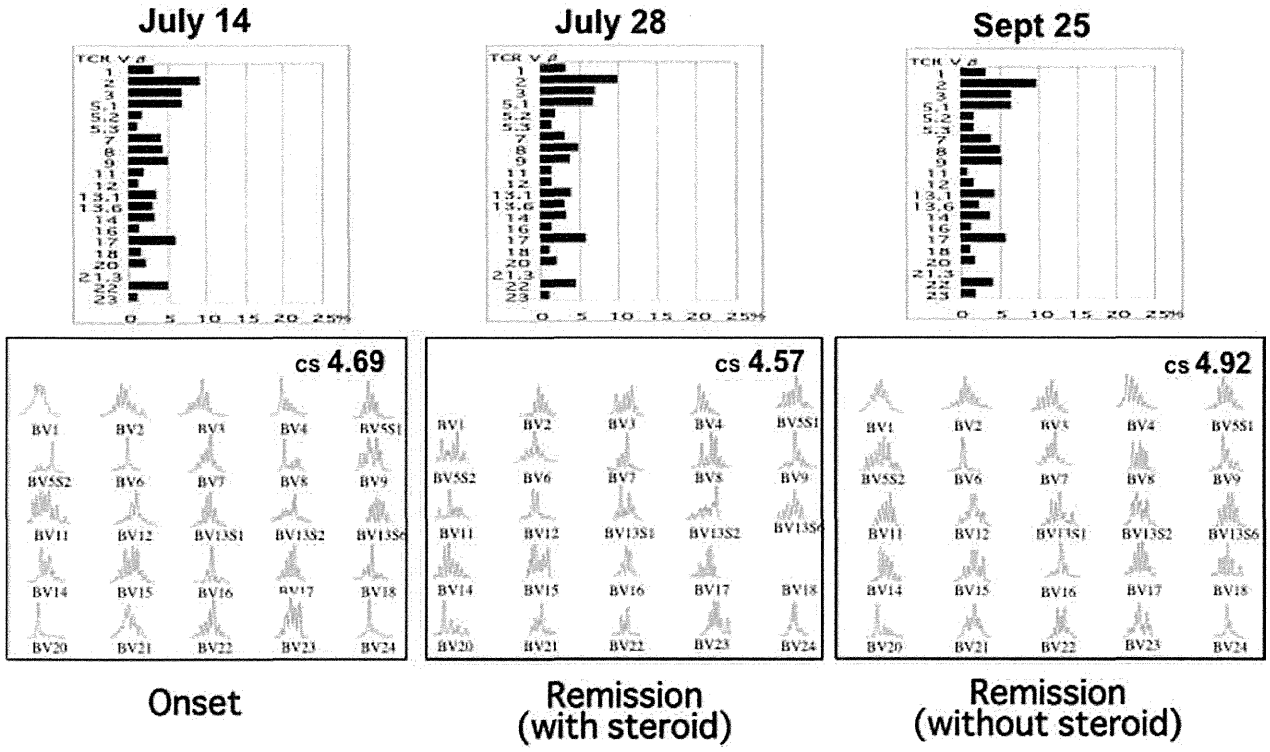

Figure 7. Effect of short-term steroid therapy on CD8+ TCR diversity. Short-term steroid therapy did not result in significant distortion of the TCR repertoire or CDR3 size distribution. CS values were 4.69 at onset, 4.57 at remission with steroid and 4.92 at remission without steroid.

initially a FR and the mean CS value was very low (4.02) at onset. After 3 years of therapy, and with improved clinical symptoms, mean CS value had improved to 4.92. Representative CDR3 size distribution profiles are shown for selected TCR Vβ repertoires.

Combined qualitative and quantitative analyses of TCR repertoires in MCNS patients

An improved visual representation is achieved by combining the results of TCR Vβ repertoire distribution and CDR3 size distribution analyses, allowing analysis of sequential changes in TCR diversity. In normal controls and NFRs, all Vβ repertoires in $CD8^+$ T cells showed a Gaussian distribution. In FRs/SD patients, however, selected Vβ repertoires in $CD8^+$ T cells were markedly increased and CDR3 size analysis showed an oligoclonal and/or monoclonal pattern. These findings were emphasized to a greater degree in the 3-dimensional views and the expansion of oligoclonal $CD8^+$ T cells was more readily appreciated (Figure 9). These expanded oligoclonal and/or monoclonal CD8+ T cells appeared to be involved in the degree of intractability of MCNS. However, we were unable to confirm the specific clone for MCNS.

Discussion

MCNS is the most frequently encountered glomerular disease in childhood, and is characterized by massive proteinuria, hypoalbuminemia, hyperlipidemia, and edema. As the name implies, minimal structural abnormality is detectable under light microscopy, but the characteristic finding of podocyte fusion involving glomerular epithelial cells is seen under electron microscopy. Steroids are generally effective in a large proportion of patients with MCNS, with ~ 90% of pediatric patients with MCNS responding to steroid therapy, and ~ 40% of those responders remaining disease-free without relapses [1, 2]. However, 20% of pediatric patients with MCNS are FRs, and 30% are SD [1, 2]. In such FRs/SD patients, the side effects of long-term steroid therapy become an important problem. Various effective immunosuppressive agents including cyclosporine have

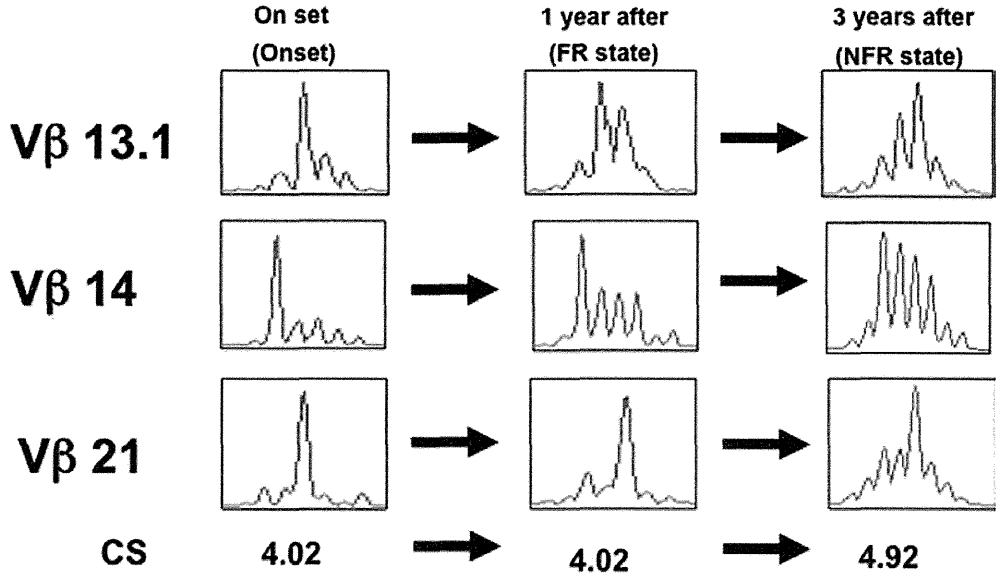

Figure 8. Relationship between clinical course and change in $CD8^+$ TCR diversity. The increase in CS correlated well with improvements in clinical course.

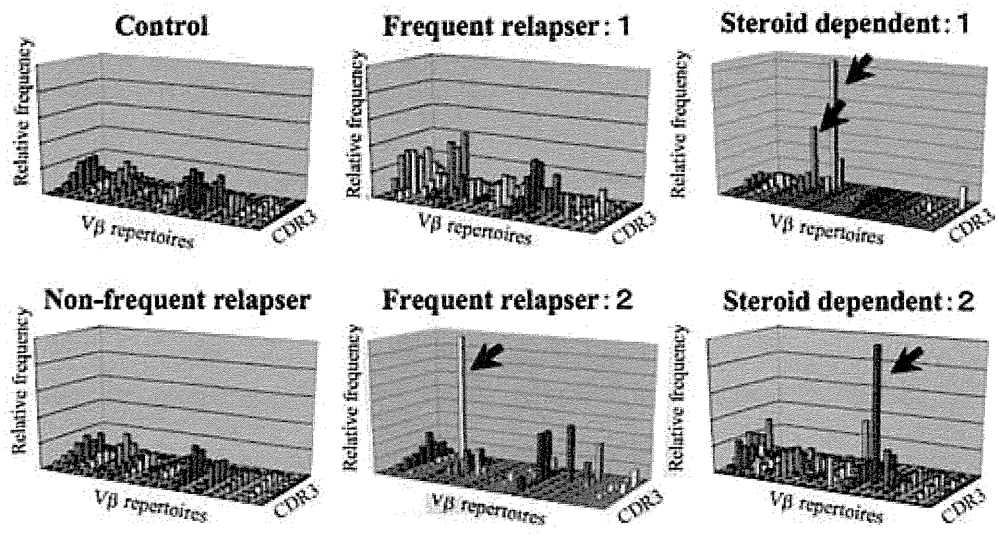

Figure 9. Three-dimensional analysis of $CD8^+$ TCR repertoires in each group of MCNS patients. In FRs/SD patients, selected Vβ repertoires in $CD8^+$ T cells were markedly increased and CDR3 size analysis showed oligoclonal and/or monoclonal patterns.

recently been used in the treatment of MCNS [7]. However, oral steroids are the drugs of choice for initial treatment of MCNS in most cases, and immunosuppressive agents are rarely used from the start of therapy. Cyclosporine can be selected as an alternative if response to steroids is absent or insufficient. Various side effects of long-term steroid therapy are usually apparent when cyclosporine is started. For this reason, the ability to predict steroid-responsiveness before starting initial therapy for MCNS patients would be advantageous. If this were possible, immunosuppressive agents such as cyclosporine could be used for FRs/SD patients from the early stages of the disease. Early introduction of immunosuppressive therapy for selected patients might successfully minimize adverse effects of steroids and improve the prognosis of MCNS.

In 1974, Shalhoub [3] proposed that certain circulating lymphokines might act as toxic agents affecting the glomerular filtration barrier in MCNS, and that the disease was an immune-mediated disorder caused by a single mechanism. Since then, a number of studies

have shown various immunological abnormalities in this disease. Activated $CD4^+$ T cells were found to be upregulated during the active stages of the disease, producing increased levels of interleukin-2. Moreover, the $CD4^+/CD8^+$ ratio was observed to be inverted, suggesting increased cytotoxic T-cell recruitment during the active stage. Such findings strongly suggested that T cells play a major role in the pathogenesis of MCNS [4, 5].

TCR diversity has recently been analyzed in various illnesses such as collagen-vascular diseases, immunodeficiency disorders, and lymphoid malignancies [17, 18, 19, 20, 21, 22]. One report provided strong evidence for direct involvement of $CD8^+$ T cells in the complicated course of idiopathic nephrotic syndrome [21]. Another report conversely demonstrated that the recurrence of idiopathic nephrotic syndrome after transplantation does not involve TCR activation or specific clonal expansion of T cells [22]. Few additional studies have elucidated the role of T cells in the pathogenesis of nephrotic syndrome. The present study compared TCR diversity profiles by analyzing the distributions of CDR3 sizes and Vβ repertoires in three different clinical groups of pediatric MCNS patients. In NFRs, abnormalities in Vβ repertoire distribution were rare in both $CD4^+$ and $CD8^+$ T cells. In many FRs/SD patients, TCR diversity was significantly reduced in $CD8^+$ T cells, as shown by the distortion of Vβ repertoire distributions and the skewing of CDR3 size distributions. Skewing of CDR3 size distributions was more marked than the distortion of Vβ repertoire distributions in $CD8^+$ T cells from these patients. The results suggest that the appearance of small numbers of oligoclonal $CD8^+$ T cells may precede the massive expansion of clones that become detectable by flow cytometry as representing a sizable fraction of TCR Vβ subfamilies. The 3-dimensional landscape view of TCR diversity allows better visualization of the subtle changes in these parameters and provides fast and easy recognition of skewed TCR patterns. Based on the abovementioned results, TCR diversity of $CD8^+$ T cells was recognized to have been lost in intractable MCNS. However, in this study we were unable to determine whether the loss of TCR diversity in $CD8^+$ T cells was part of the etiology of MCNS or a simple result.

Significant improvement in $CD8^+$ T-cell TCR diversity was observed in selected FRs who showed gradual improvements in their clinical course. Furthermore, short-term steroid therapy may not induce skewing of TCR diversity, as profiles did not change significantly in one of the patients. These findings indicate that the significant skewing of TCR diversity is not a result of steroid therapy. While we did not perform investigations for other immunosuppressive drugs, the results seem likely to be similar in the short term. Skewing of TCR diversity may directly reflect the pathogenic role played by the expanding oligoclonal T cells in pediatric MCNS. In this regard, TCR diversity in $CD8^+$ T cells, particularly in the form of mean CS values in $CD8^+$ T cells, may serve as a good clinical parameter, and analysis of TCR diversity may allow delineation of the subgroup of patients most likely to benefit from early intervention with immunosuppressive therapy. If immunosuppressive therapy could be introduced early for those patients, both clinical response and quality of life might be markedly improved.

Further investigation is necessary to confirm our hypothesis. We do not know whether our findings apply only to pediatric patients or whether they also hold true for adult patients. Indeed, whether the analysis of TCR structure is truly useful for the prediction of disease outcome remains unclear. To answer these questions, prospective studies are currently being planned to compare clinical responses and outcomes in patients with the results of TCR diversity analyses. Furthermore, this study was unable to examine TCR diversity profiles in patients with steroid-resistant nephrotic syndrome. We thus hope to add similar examinations of TCR diversity for patients with steroid-resistant nephrotic syndrome in future investigations.

Acknowledgment

This work supported by a Grant-in-Aid for Scientific Research (c) from the Japan Society for the Promotion of Science (JSPS) and by a Grant from the Ministry of Health, Labor, and Welfare of Japan.

References

[1] *International Study of Kidney Disease in Children.* Nephrotic syndrome in children: prediction of histopathology from clinical and laboratory characteristics at time of diagnosis. A report of the International Study of Kidney Disease in Children. Kidney Int. 1978; *13:* 159-165. doi:10.1038/ki.1978.23 PubMed

[2] *Niaudet P.* Steroid-sensitive idiopathic nephrotic syndrome in children. In: Avner ED, Harmon WE, Niaudet P (eds). Pediatric Nephrology, ed 5. Philadelphia: Lippincott Williams & Wilkins; 2004. p. 543-556.

[3] *Shalhoub RJ.* Pathogenesis of lipoid nephrosis: a disorder of T-cell function. Lancet. 2004; *2:* 556-560.

[4] *Cunard R, Kelly CJ.* T cells and minimal change disease. J Am Soc Nephrol. 2002; *13:* 1409-1411. doi:10.1097/01.ASN.0000016406.82019.B3 PubMed

[5] *Lama G, Luongo I, Tirino G, Borriello A, Carangio C, Salsano ME.* T-lymphocyte populations and cytokines in childhood nephrotic syndrome. Am J Kidney Dis. 2002; *39:* 958-965. doi:10.1053/ajkd.2002.32769 PubMed

[6] *Patrakka J, Lahdenkari AT, Koskimies O, Holmberg C, Wartiovaara J, Jalanko H.* The number of podocyte slit diaphragms is decreased in minimal change nephrotic syndrome. Pediatr Res. 2002; *52:* 349-355. PubMed

[7] *Eddy AA, Symons JM.* Nephrotic syndrome in childhood. Lancet. 2003; *362:* 629-639. doi:10.1016/S0140-6736(03)14184-0 PubMed

[8] *Konno A, Okada K, Mizuno K, Nishida M, Nagaoki S, Toma T, Uehara T, Ohta K, Kasahara Y, Seki H, Yachie A, Koizumi S.* CD8alpha alpha memory effector T cells descend directly from clonally expanded CD8alpha + beta high TCRalpha β T cells in vivo. Blood. 2002; *100:* 4090-4097. doi:10.1182/blood-2002-04-1136 PubMed

[9] *Mizuno K, Yachie A, Nagaoki S, Wada H, Okada K, Kawachi M, Toma T, Konno A, Ohta K, Kasahara Y, Koizumi S.* Oligoclonal expansion of circulating and tissue-infiltrating CD8+ T cells with killer/effector phenotypes in juvenile dermatomyositis syndrome. Clin Exp Immunol. 2004; *137:* 187-194. doi:10.1111/j.1365-2249.2004.02500.x PubMed

[10] *Chomczynski P, Sacchi N.* Single-step method of RNA isolation by acid guanidinium thiocyanate-phenol-chloroform extraction. Anal Biochem. 1987; *162:* 156-159. doi:10.1016/0003-2697(87)90021-2 PubMed

[11] *Choi YW, Kotzin B, Herron L, Callahan J, Marrack P, Kappler J.* Interaction of *Staphylococcus aureus* toxin "superantigens" with human T cells. Proc Natl Acad Sci USA. 1989; *86:* 8941-8945. doi:10.1073/pnas.86.22.8941 PubMed

[12] *Labrecque N, McGrath H, Subramanyam M, Huber BT, Sékaly RP.* Human T cells respond to mouse mammary tumor virus-encoded superantigen: V beta restriction and conserved evolutionary features. J Exp Med. 1993; *177:* 1735-1743. doi:10.1084/jem.177.6.1735 PubMed

[13] *Bomberger C, Singh-Jairam M, Rodey G, Guerriero A, Yeager AM, Fleming WH, Holland HK, Waller EK.* Lymphoid reconstitution after autologous PBSC transplantation with FACS-sorted CD34+ hematopoietic progenitors. Blood. 1998; *91:* 2588-2600. PubMed

[14] *Zeng W, Nakao S, Takamatsu H, Yachie A, Takami A, Kondo Y, Sugimori N, Yamazaki H, Miura Y, Shiobara S, Matsuda T.* Characterization of T-cell repertoire of the bone marrow in immune-mediated aplastic anemia: evidence for the involvement of antigen-driven T-cell response in cyclosporine-dependent aplastic anemia. Blood. 1999; *93:* 3008-3016. PubMed

[15] *Pilch H, Höhn H, Freitag K, Neukirch C, Necker A, Haddad P, Tanner B, Knapstein PG, Maeurer MJ.* Improved assessment of T-cell receptor (TCR) VB repertoire in clinical specimens: combination of TCR-CDR3 spectratyping with flow cytometry-based TCR VB frequency analysis. Clin Diagn Lab Immunol. 2002; *9:* 257-266. PubMed

[16] *Yawalkar N, Ferenczi K, Jones DA, Yamanaka K, Suh KY, Sadat S, Kupper TS.* Profound loss of T-cell receptor repertoire complexity in cutaneous T-cell lymphoma. Blood. 2003; *102:* 4059-4066. doi:10.1182/blood-2003-04-1044 PubMed

[17] *Namekawa T, Wagner UG, Goronzy JJ, Weyand CM.* Functional subsets of CD4 T cells in rheumatoid synovitis. Arthritis Rheum. 1998; *41:* 2108-2116. doi:10.1002/1529-0131(199812)41:12<2108::AID-ART5>3.0.CO;2-Q PubMed

[18] *Cherin P, Herson S, Crevon MC, Hauw JJ, Cervera P, Galanaud P, Emilie D.* Mechanisms of lysis by activated cytotoxic cells expressing perforin and granzyme-B genes and the protein TIA-1 in muscle biopsies of myositis. J Rheumatol. 1996; *23:* 1135-1142. PubMed

[19] *Rieux-Laucat F, Bahadoran P, Brousse N, Selz F, Fischer A, Le Deist F, De Villartay JP.* Highly restricted human T cell repertoire in peripheral blood and tissue-infiltrating lymphocytes in Omenn's syndrome. J Clin Invest. 1998; *102:* 312-321. doi:10.1172/JCI332 PubMed

[20] *O'Shea UD, Hollowood KM, Boylston AW.* Demonstration of the oligoclonality of an enteropathy associated T-cell lymphoma by monoclonal antibodies and PCR analysis of the T-cell receptor V-beta repertoire on fixed tissue. Hum Pathol. 1996; *27:* 509-513. doi:10.1016/S0046-8177(96)90095-7 PubMed

[21] *Frank C, Herrmann M, Fernandez S, Dirnecker D, Böswald M, Kolowos W, Ruder H, Haas JP.* Dominant T cells in idiopathic nephrotic syndrome of childhood. Kidney Int. 2000; *57:* 510-517. doi:10.1046/j.1523-1755.2000.00870.x PubMed

[22] *Hervé C, Le Berre L, Miqueu P, Degauque N, Ruiz C, Brouard S, Guillet M, Soulillou JP, Dantal J.* Blood T-cell repertoire in idiopathic nephrotic syndrome recurrence following kidney transplantation. Am J Transplant. 2006; *6:* 2144-2151. doi:10.1111/j.1600-6143.2006.01415.x PubMed

TRAM Is Involved in IL-18 Signaling and Functions as a Sorting Adaptor for MyD88

Hidenori Ohnishi[1]*, Hidehito Tochio[2]*, Zenichiro Kato[1], Norio Kawamoto[1], Takeshi Kimura[1], Kazuo Kubota[1], Takahiro Yamamoto[1], Tatsuyoshi Funasaka[3], Hiroshi Nakano[3], Richard W. Wong[3], Masahiro Shirakawa[2], Naomi Kondo[1]

1 Department of Pediatrics, Graduate School of Medicine, Gifu University, Gifu, Japan, **2** Department of Molecular Engineering, Graduate School of Engineering, Kyoto University, Kyoto, Japan, **3** Laboratory of Molecular and Cellular Biology, Department of Biology, School of Natural System, Kanazawa University, Kakuma-machi, Kanazawa, Japan

Abstract

MyD88, a Toll/interleukin-1 receptor homology (TIR) domain-containing adaptor protein, mediates signals from the Toll-like receptors (TLR) or IL-1/IL-18 receptors to downstream kinases. In MyD88-dependent TLR4 signaling, the function of MyD88 is enhanced by another TIR domain-containing adaptor, Mal/TIRAP, which brings MyD88 to the plasma membrane and promotes its interaction with the cytosolic region of TLR4. Hence, Mal is recognized as the "sorting adaptor" for MyD88. In this study, a direct interaction between MyD88-TIR and another membrane-sorting adaptor, TRAM/TICAM-2, was demonstrated *in vitro*. Cell-based assays including RNA interference experiments and TRAM deficient mice revealed that the interplay between MyD88 and TRAM in cells is important in mediating IL-18 signal transduction. Live cell imaging further demonstrated the co-localized accumulation of MyD88 and TRAM in the membrane regions in HEK293 cells. These findings suggest that TRAM serves as the sorting adaptor for MyD88 in IL-18 signaling, which then facilitates the signal transduction. The binding sites for TRAM are located in the TIR domain of MyD88 and actually overlap with the binding sites for Mal. MyD88, the multifunctional signaling adaptor that works together with most of the TLR members and with the IL-1/IL-18 receptors, can interact with two distinct sorting adaptors, TRAM and Mal, in a conserved manner in a distinct context.

Citation: Ohnishi H, Tochio H, Kato Z, Kawamoto N, Kimura T, et al. (2012) TRAM Is Involved in IL-18 Signaling and Functions as a Sorting Adaptor for MyD88. PLoS ONE 7(6): e38423. doi:10.1371/journal.pone.0038423

Editor: Tianyi Wang, University of Pittsburgh, United States of America

Received February 8, 2012; **Accepted** May 9, 2012; **Published** June 7, 2012

Funding: This work was supported by Grants-in-Aid for Scientific Research from the Ministry of Education, Sports Science, Culture and Technology of Japan and by Health and Labour Science Research Grants for Research on Intractable Disease from the Ministry of Health, Labour and Welfare, Japan. The funders had no role in study design, data collection and analysis, decision to publish, or preparation of the manuscript.

Competing Interests: The authors have declared that no competing interests exist.

* E-mail: ohnishih@gifu-u.ac.jp (HO); tochio@moleng.kyoto-u.ac.jp (HT)

Introduction

Toll-like receptors (TLRs) are representative innate immune receptors that recognize pathogen-associated molecular patterns (PAMPs). MyD88, a cytosolic adaptor protein, is involved in the signaling pathways initiated by all of the reported TLRs with the exception of TLR3 [1]. Usually, PAMPs first bind to the extracellular domain of the TLRs, and the cytosolic region of TLRs then interact with MyD88, which allows the signal to be transmitted to the downstream kinase Interleukin (IL) -1 receptor associated kinase 4 (IRAK4). The resulting activation of IRAK4 eventually leads to the activation of the transcription factors NF-κB and AP-1 via conserved phosphorylation cascades [2]. MyD88 is composed of two functional domains: an N-terminal death domain (DD) and a C-terminal Toll/Interleukin-1 receptor homology (TIR) domain [3]. The DD is a protein interaction module that is involved in a variety of cellular events. Similar to the DD, the TIR domain also mediates protein-protein interactions via homotypic TIR-TIR interactions. In contrast to the DD, the TIR domain is almost exclusively found in the TLR related cytosolic adaptors or in the cytosolic regions of the TLRs, IL-1 and IL-18 receptors. Homotypic interactions of these protein interaction modules play a pivotal role in transmitting the signals downstream from the TLR; the TIR of MyD88 interacts with the TIR of the TLRs, and the DD of MyD88 interacts with the DD of IRAK4, which forms a large protein complex called the Myddosome [4].

TLR4 signaling, the best characterized signaling pathway among a dozen of known TLR pathways, is activated by lipopolysaccharide (LPS) from gram-negative bacteria, and the pathway plays a major role in endotoxin shock. Two modes of the signaling have been described: the MyD88-dependent and MyD88-independent pathways. In the MyD88-dependent TLR4 signal transduction pathway, another TIR domain-containing adaptor protein, Mal (also called TIRAP), plays an important role. Mal binds MyD88 via a homotypic TIR interaction and then associates with the plasma membrane using its PIP2-binding domain. Thus, Mal has been suggested to serve as a "sorting adaptor" that recruits the "signaling adaptor", MyD88, to the membrane region where the activated TLR4 resides [5]. Mal is not an essential factor for the signaling because signal transduction can occur even without Mal [6,7], but Mal can substantially facilitate the signaling. A pair of TIR domain-containing adaptors, TIR domain-containing adaptor inducing IFN-β (TRIF) and TRIF-related adaptor molecule (TRAM), is known to play important roles in the MyD88-independent TLR4-signaling

pathway in which TRIF and TRAM function as the signaling and the sorting adaptors, respectively. This pathway transmits signals from TLR4 at early endosomes after the LPS-induced internalization of TLR4 [8,9]. TRAM is known to deliver TRIF to the endosomes via a specific region of the plasma membrane by using its myristoylation site and polybasic region [10]. These findings indicate that the specific combinations of the sorting and the signaling TIR-containing adaptors define the specific signal transduction pathways.

MyD88 is also involved in acquired immune responses because it mediates the signals from the inflammatory cytokines IL-1 and IL-18; ligand-activated IL-1/IL-18 receptors that subsequently interact with MyD88 to trigger downstream protein kinase cascades that eventually activate the transcription factors NF-κB and AP-1 in a similar manner to TLR signaling. Although the intracellular signaling pathway is similar to the MyD88-dependent TLR4 pathway, the sorting-adaptor Mal is not involved [11]. As mentioned above, TLR4 signaling is facilitated either by Mal (MyD88-dependent pathway) or TRAM (MyD88-independent pathway) in a pathway-dependent manner. The former mainly localizes in PIP2 rich plasma membrane regions, while the latter is found not only in the plasma membrane but also in the internalized early endosomes that dispatch the signals. Thus, different sorting adaptors recruit MyD88 to different membrane regions and create distinct types of signal initiation complexes. In contrast to TLR signals, IL-1/IL-18 signaling has not thus far been thought to require such sorting adaptors. Interestingly, Kagan *et al.* reported that an engineered MyD88 that is endowed with PIP2 binding ability could rescue the LPS-TLR4 signaling in mouse embryonic fibroblast (MEF) cells from MyD88 and Mal double knockout mice, although it failed to rescue IL-1 signaling in the cells [5]. This observation suggests that TLR4 and IL-1R are located in distinct regions of the plasma membrane, which then raises the hypothesis that unidentified sorting adaptors selectively bring MyD88 to the appropriate membrane region to form signal initiation complexes with activated IL-1 and IL-18 receptors.

In this study, we sought the sorting adaptor for IL-18 signaling and discovered that TRAM is responsible for this function. TRAM was demonstrated to directly interact with MyD88 in *in vitro* binding experiments in which a homotypic TIR-TIR interaction plays a vital role. The efforts to identify the interacting sites in the MyD88-TIR interaction revealed that two surface sites of MyD88-TIR are direct interfaces with TRAM-TIR. Interestingly, these interaction sites overlap with the sites for Mal binding [12]. Furthermore, cellular assays demonstrated the functional involvement of TRAM in the IL-18 signal transduction, and TRAM changed the localization of MyD88 from the cytosol to the membranous regions. These new findings strongly suggest that TRAM is the membrane-sorting adaptor for MyD88 in IL-18 signaling and plays a critical role in transmitting the signal. Thus, the mechanism of signal initiation is more conserved between the MyD88-dependent TLR4 pathway and IL-18 signaling than previously thought.

Results

Binding of TRAM to MyD88

Five TIR containing adaptor proteins have been previously identified: MyD88, Mal, TRIF, TRAM and SARM. Mal and TRAM were reported to be the sorting adaptors for MyD88 and TRIF, respectively [13]. Because a model structure of the TIR domain of TRAM represents a substantially large negatively charged surface area (Figure S1), while the TIR domain of MyD88 is covered by positive charge, we expected some interaction between these two adaptor molecules. We thus further hypothesized that TRAM also functions as the sorting adaptor for MyD88 in the IL-18 signaling pathway. To test these ideas, we first examined the direct interaction between MyD88 and TRAM. As both of the adaptors contain the TIR domain, which mediates the protein-protein interaction generally via homomeric or heteromeric TIR-TIR interactions, the direct interaction between the MyD88-TIR and the TRAM-TIR was examined with a GST-pull down assay. The results indicated that the wild-type MyD88-TIR directly bound the TRAM-TIR with a higher affinity than Mal, while the interaction between MyD88-TIR and TLR1-TIR, which had been shown not to bind the MyD88-TIR [14], was not detected in this method (Figure 1A). We then examined the interaction between MyD88 and TRAM in cells using a co-immunoprecipitation analysis. When Myc-MyD88 and FLAG-TRAM were co-expressed in HEK293 cells, the Myc-MyD88 constitutively associated with the FLAG-TRAM (Figure 2), which is consistent with our GST-pull down assay. Strikingly, upon stimulation of the cells with IL-18, the MyD88-TRAM complex gradually dissociated over a 30- to 120-minute time course. The HEK293 cells inherently express IL-18Rα (formerly called IL-1Rrp), which is a necessary component for IL-18 signaling, but lack IL-18Rβ (formerly called IL-1AcPL). Thus, we additionally co-expressed IL-18Rβ in the cells for this experiment.

Binding of TRAM to IL-18 Receptors

For the activation of IL-18 signaling, the heterodimerization of two IL-18 receptors, IL-18Rα and IL-18Rβ, has been shown to be required [15]. These receptors belong to the IL-1 receptor superfamily and are thus structurally homologous to one another. The extracellular region contains immunoglobulin (Ig)-like chains, while the cytosolic region has a TIR domain that interacts with the TIR domain of MyD88. To test the interaction of TRAM with these IL-18 receptors, we performed GST pull-down assays using the TIR domains of the IL-18 receptors and TRAM. The results showed that the TIR domains from both IL-18Rα and IL-18Rβ directly bound the TRAM-TIR (Figure 1B).

Involvement of TRAM in IL-18 Signaling

After obtaining the evidence that TRAM interacts with MyD88 both *in vitro* and in cells, we then examined the possible involvement of TRAM in IL-18 signaling. We knocked-down the endogenous TRAM expression in HEK293 cells using siRNA techniques and then performed NF-κB reporter assays for the IL-18 signal transduction in the cells. The shRNA for the TRAM expressing vector was generated based on the previously reported target sequence [16]. When the expression of TRAM was knocked-down (Figure 3A), NF-κB activity after IL-18 stimulation was markedly decreased relative to the negative control experiments that used scrambled shRNA (Figure 3B). This result indicates that the knock-down of TRAM expression actually impaired the IL-18 signal transduction. We confirmed the knock-down effect of this shRNA sequence for TRAM via the LPS-stimulated activation of IFN-β promoter, which is presumably due to the suppression of the MyD88-independent TLR4 pathway mediated by TRAM and TRIF (Figure 3C). The effect was similar when compared to the results obtained from a dominant negative form of TRAM (C117H). TRAM (C117H) showed an almost complete shutdown of the LPS/TLR4/IFN-β signaling in the cells (Figure 3D) and the decrease of the enhancement of NF-κB activity induced by IL-18 (Figure 3E). To further confirm the involvement of TRAM in the IL-18 signaling pathway, we evaluated the cytokine production from helper type 1 differentiated T (Th1) cells isolated from TRAM-deficient mice and

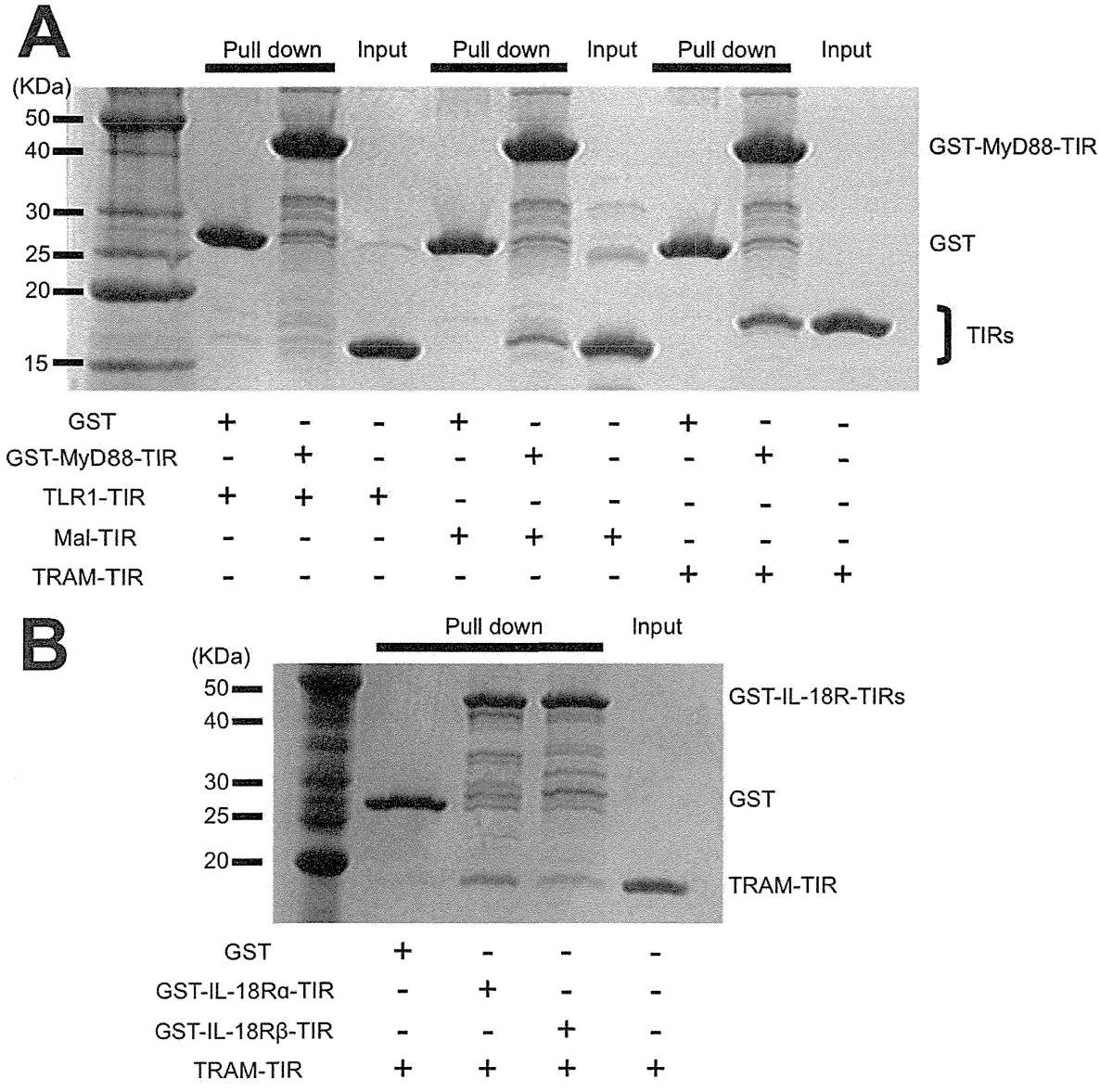

Figure 1. Protein interaction assays. (A) GST pull-down assay investigating the direct interactions between the GST-MyD88-TIR and the TRAM-TIR or TLR1-TIR. (B) GST pull-down assay between the GST-IL-18 receptor TIRs and TRAM-TIR.
doi:10.1371/journal.pone.0038423.g001

MyD88-deficient mice. IL-18 did not produce IFN-γ from not only MyD88-deficient Th1 cells but also TRAM-deficient Th1 cells, significantly. And, IL-18 alone or IL-18 and IL-12 co-stimulated TRAM-deficient Th1 cells produced significantly lower IFN-γ levels than those of wild-type Th1 cells (Figure 4).

IL-18 Modulates MyD88-TRAM Subcomplex in Human Cells

Next, we further investigated whether MyD88 actually interacted with TRAM in human HEK293T cells by live cell fluoroimaging. When we transiently transfected a DsRed-TRAM construct into HEK293T cells, the protein localized to the plasma membrane region, which was consistent with a previous report [10] (Figure 5A). In contrast, GFP-MyD88 was dominantly found as foci in the cytosol in the cells expressing the protein; this has also been shown by others [17] (Figure 5B). Strikingly, when HEK293T cells were co-transfected with expression plasmids for GFP-MyD88 and DsRed-TRAM, MyD88 proteins moderately co-localized with TRAM in the membrane regions (Figure 5C). These data strongly suggest that this transient interaction between the two proteins dramatically altered the localization of GFP-MyD88 from the cytosol to the membranes. Thus, TRAM both bound and endowed MyD88 with membrane targeting properties as has been previously demonstrated for Mal [5].

Identification of Important Amino Acid Residues of the MyD88-TIR in IL-18 Signaling

Having established that MyD88 and TRAM directly interact and that the interaction is critical in IL-18 signaling, we next carried out experiments to identify the amino acid residues of MyD88 that are important in this interaction. A cell-based reporter assay system was utilized to examine various mutations in

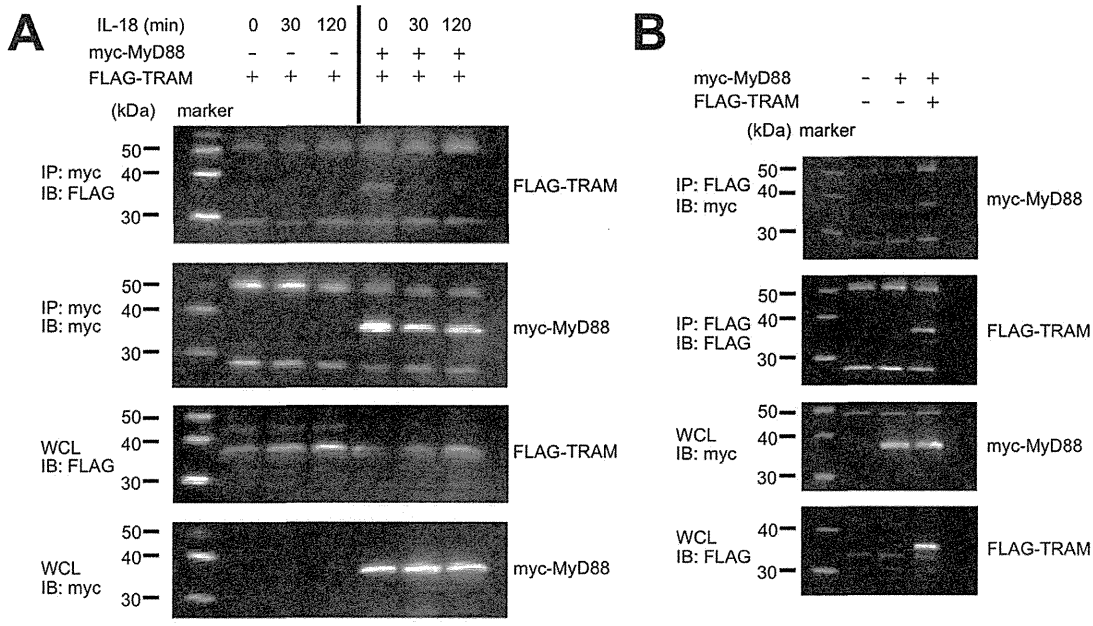

Figure 2. Assay of the interaction between MyD88 and TRAM in IL-18 signaling. (A) MyD88 and TRAM were co-expressed in HEK293T cells along with IL-18Rβ. IL-18 stimulation was carried out as indicated. MyD88 was immunoprecipitated using the Myc-tag antibody; co-immunoprecipitated TRAM was also detected. (B) The opposite direction co-immunoprecipitation assay between MyD88 and TRAM. Myc-MyD88 was detected with immunoprecipitated FLAG-TRAM.
doi:10.1371/journal.pone.0038423.g002

the MyD88-TIR as previously reported [12]. The results are shown in Figure 6A. An alanine substitution of any one of eight residues (Arg196, Asp197, Lys214, Arg217, Lys238, Arg269, Lys282 or Arg288) caused significantly reduced dominant negative inhibitory effects on IL-18 signaling indicating that these residues are involved in the signal transduction. These eight residues are mapped on the protein structure of the MyD88-TIR (PDB code: 2z5v) (Figure 6B). In our previous experiments for LPS/TLR4 signaling using the same luciferase reporter system, three discrete functional sites were found on the surface of the MyD88-TIR, which we designated Site I, Site II, and Site III (Figure 6B) [12]. Five out of the eight residues, Arg196 (Site II), Asp197 (Site II), Arg217 (Site I), Lys282 (Site III) or Arg288 (Site III) were previously found to be important in the LPS/TLR4 signaling. We then examined the direct binding of the representative mutants of each functional sites of MyD88-TIR to the TRAM-TIR using GST pull-down assays (Figure 6C). The results indicate that the binding between the MyD88-TIR and TRAM-TIR is dependent on Sites II and III because the alanine substitution of either Arg196 or Arg288 resulted in decreased binding. Furthermore, the interaction between the MyD88-TIR and TRAM-TIR was completely abrogated when both Arg196 and Arg288 were mutated. Additionally, co-immunoprecipitation assay also showed the reduction of interaction between MyD88 R196A-R288A mutant and TRAM (Figure 6D). In contrast, a Site I mutant, R217A, did not show a significant decrease in binding affinity. Overall, these interactions are very similar to those observed between the MyD88-TIR and Mal-TIR [12], indicating that TRAM and Mal share the same binding sites on MyD88-TIR.

Discussion

Involvement of TRAM in the IL-18 Pathway

Mal has been reported to function as the sorting adaptor in the TLR4 signaling that brings MyD88 to the plasma membrane to mediate the interactions between TLR4 and MyD88 [5]. Because the IL-1 and IL-18 receptors also form signal initiation complexes that contain MyD88, presumably at distinct membrane regions from TLR4, the existence of currently unidentified sorting adaptors that recruit MyD88 to specific membrane regions and mediate the interactions between MyD88 and the IL-1/IL-18 receptors has been hypothesized [5]. Although several reports have been published to date, the involvement of TRAM in IL-1 signaling remains controversial [16,18,19,20]. Using TRAM-deficient mice, Yamamoto *et al.* showed that TRAM is not involved in IL-1 signaling. Despite the homology between IL-1 and IL-18, the relationship between TRAM and IL-18 had not yet been elucidated. In this study, we sought the sorting adaptor that acts in IL-18 signaling and found that TRAM fulfils this role. It was proposed that the electric potential is important for the specific interactions between the TIR domain proteins [21]. According to the electric surface potentials of the TIR domain structures, the TRAM-TIR and Mal-TIR both have a largely acidic surface patch, while the MyD88-TIR has a largely basic surface patch (Figure S1). Therefore we hypothesized that TRAM interacts with MyD88 and works as the sorting adaptor that recruits MyD88 in IL-18 signaling. In fact, TRAM has already been reported as the sorting adaptor in the MyD88-independent TLR4 pathway in which TRAM recruits TRIF to specific membrane regions [10,22]. Nonetheless, in this work we obtained multiple results that indicate that TRAM functions as the sorting adaptor for IL-18 signals as we initially hypothesized. First, TRAM bound to MyD88 *in vitro* and in cells (Figure 1A, 2, and 5C). Second, the intracellular TIR domains of IL-18 receptors also bound to TRAM-TIR (Figure 1B). Finally, the shRNA knock-down of TRAM expression and knock-out of TRAM caused a significant decrease in the cellular response to IL-18 stimulation (Figure 3 and 4). These findings strongly suggest that TRAM functions as the sorting adaptor for MyD88 in IL-18 signaling. On

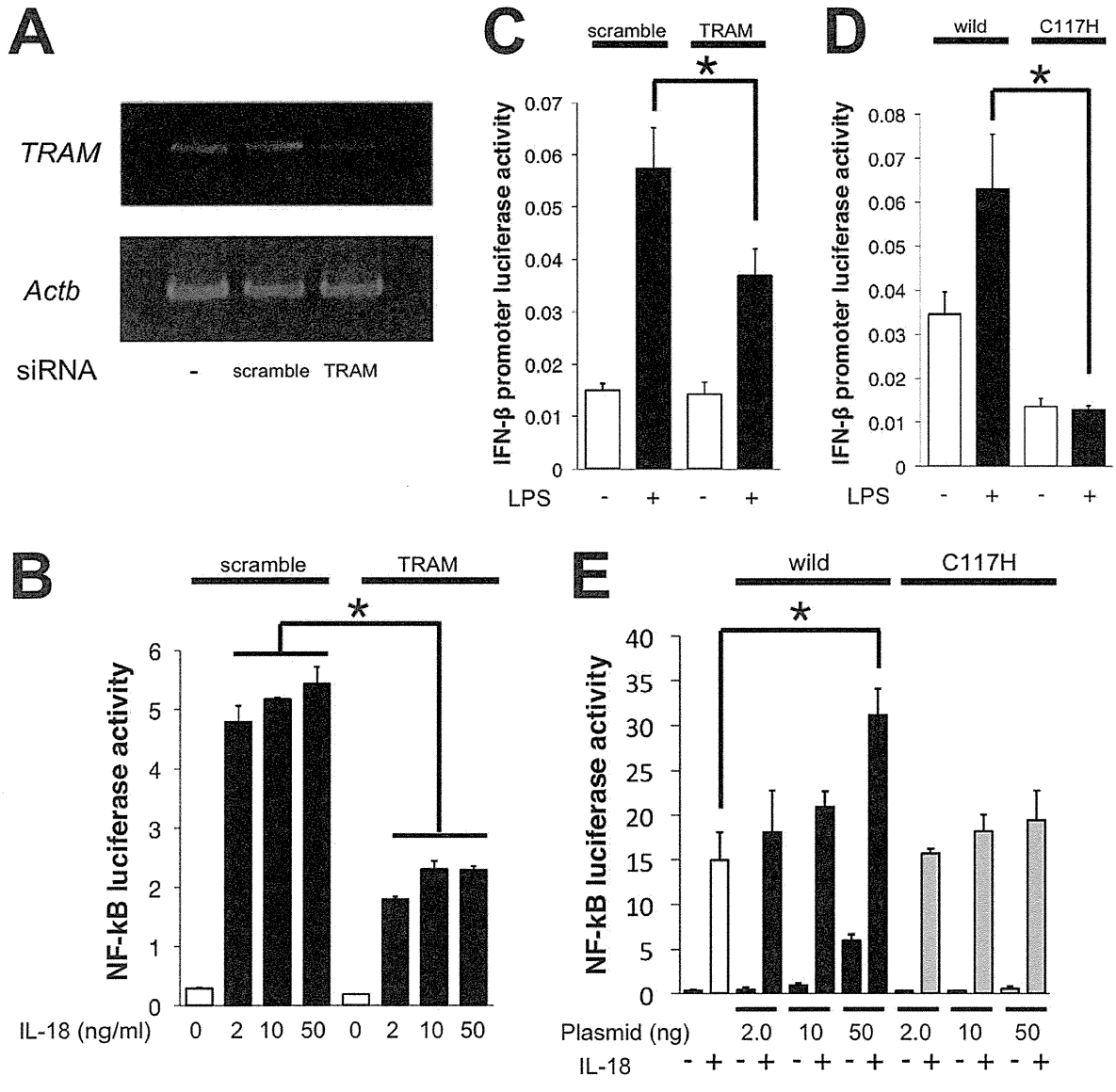

Figure 3. The knock-down effects of TRAM in IL-18 or LPS/TLR4 signaling. (A) RT-PCR of the *TRAM* mRNA knock-down in HEK293T cells by the psiRNA-TICAM-2 but not by the nonspecific scrambled sequence coded psiRNA vector. "-" indicates cells not transfected with siRNA; "*Actb*" indicates the loading control (β-actin mRNA). (B–E) The effect of the knock-down of TRAM using shRNA or the dominant negative form of TRAM (C117H) for the IL-18 or LPS induced NF-κB or IFN-β-promoter luciferase activity assay. The NF-κB and IFN-β-promoter activities with IL-18 or LPS stimulation were significantly decreased in the IL-18Rβ co-transfected HEK293T cells or HEK293-hTLR4-MD2-CD14 cells.
doi:10.1371/journal.pone.0038423.g003

the other hand, recent reports have shown that TRAM is associated not only with TLR4 but also with the TLR2 and TLR5 signaling pathways [23,24]. These findings suggest that the conventionally accepted definition of the functions of the TIR domain-containing adaptor proteins in the TLR and IL-1/18 signaling pathways should be reconsidered.

Time Dependent Change of the Interaction between MyD88 and TRAM

A particularly interesting feature we observed in this study was that the complex between Myc-MyD88 and FLAG-TRAM expressed in HEK293T cells decreased after IL-18 stimulation in a time-dependent manner (Figure 2). This observation suggests that either the rearrangement of the signal initiation complexes or the degradation of the components in the complexes is triggered by the activation of the IL-18 signaling. A similar rearrangement of the signal initiation complex has also been observed for the TLR4 pathway in a previous report; upon activation of TLR4 by LPS, TLR4 associated with MyD88 instantly, and the association was lost within 15 min [25]. Thus, such transient interactions between the receptors and adaptors and the subsequent loss of the interaction may be common to both the TLR and the IL-18 pathways especially because they utilize many of the same intracellular components. For the TLR4 complex, phosphorylation of TLR4 and Mal has been suggested to be involved in the rearrangements [25,26]. TRAM has been shown to be phosphorylated by Protein kinase C-ε (PKC-ε) upon stimulation by LPS, and the phosphorylation has been implicated in regulating the

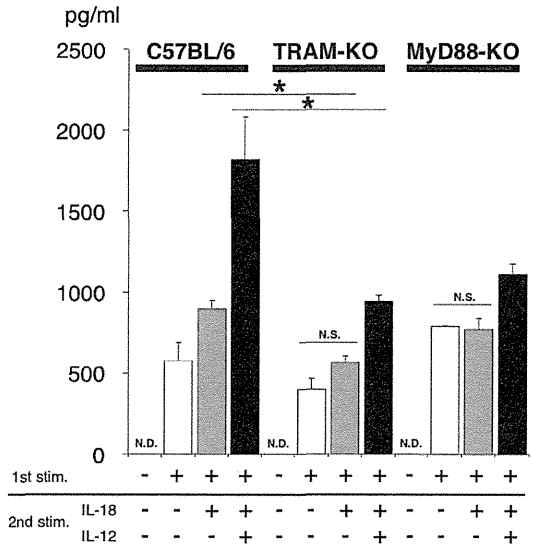

Figure 4. The IFN-γ production from IL-18 and/or IL-12 stimulated Th1 cells from TRAM-deficient mice and MyD88 deficient mice. The IFN-γ production levels were significantly reduced in TRAM deficient mice and MyD88 deficient mice. The black bars show the production levels from IL-18 and IL-12 co-stimulated Th1 cells, grey bars show those from IL-18 solely stimulated Th1 cells, and the white bars show those from no secondary stimulated Th1 cells.
doi:10.1371/journal.pone.0038423.g004

myristoylation state and thus the membrane targeting [10,27]. The membrane targeting of another myristoylated protein, MARCKS, has been shown to be regulated by phosphorylation; MARCKS is released from the plasma membrane upon the PKC mediated phosphorylation of a serine near its myristoylation site [28]. Similar to these examples, TRAM might be phosphorylated in the IL-18-induced dissociation of the MyD88-TRAM complex (Figure 2), although the mechanism underlying the dissociation and its relevance to signal regulation remain to be elucidated.

The TRAM Interaction Sites of MyD88 are Similar to that for Mal

According to our previous study [12], Sites I, II, and III on the MyD88-TIR are functionally important in TLR4 signaling. These sites also were recognized to be important in IL-18 signaling (Figure 6A and 6B). We further demonstrated that Sites II and III act as the TRAM binding sites of the MyD88 TIR domain (Figure 6C), which overlap with the Mal binding sites [12]. The two sites are distantly located from each other on opposite molecular surfaces of the protein. Because of the molecular size of the TIR domain, it is unlikely that both sites present a simultaneous binding interface for a single TRAM-TIR to form a 1:1 complex. It is more likely that each of these sites constitutes a distinct interface for a different TRAM molecule in different binding modes. Consistent with this hypothesis, a mutation of either Arg196 or Arg288 leads to only moderate losses in the binding to the TRAM-TIR in contrast to the fact that simultaneous

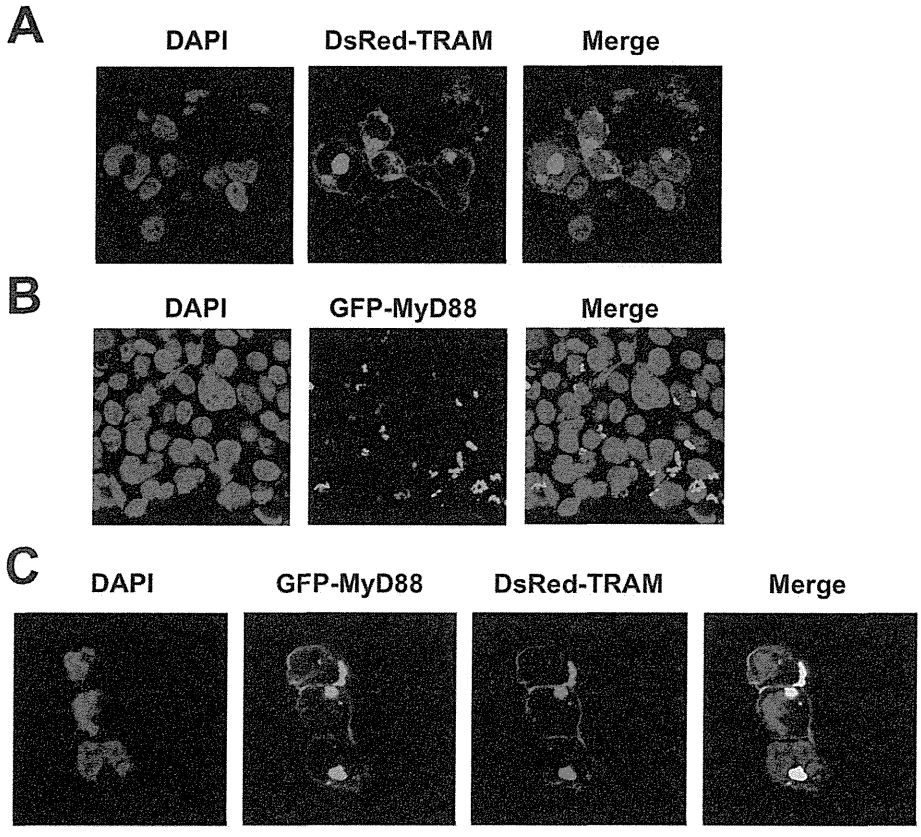

Figure 5. The localization of the MyD88 and TRAM complex in cells. (A–C) The localizations of the DsRed-TRAM (Red) and/or GFP-MyD88 (Green) in HEK293T cells. DAPI stained nuclei of HEK293T cells are shown in blue. Complexes of the DsRed fusion protein and GFP fusion protein are shown in yellow.
doi:10.1371/journal.pone.0038423.g005

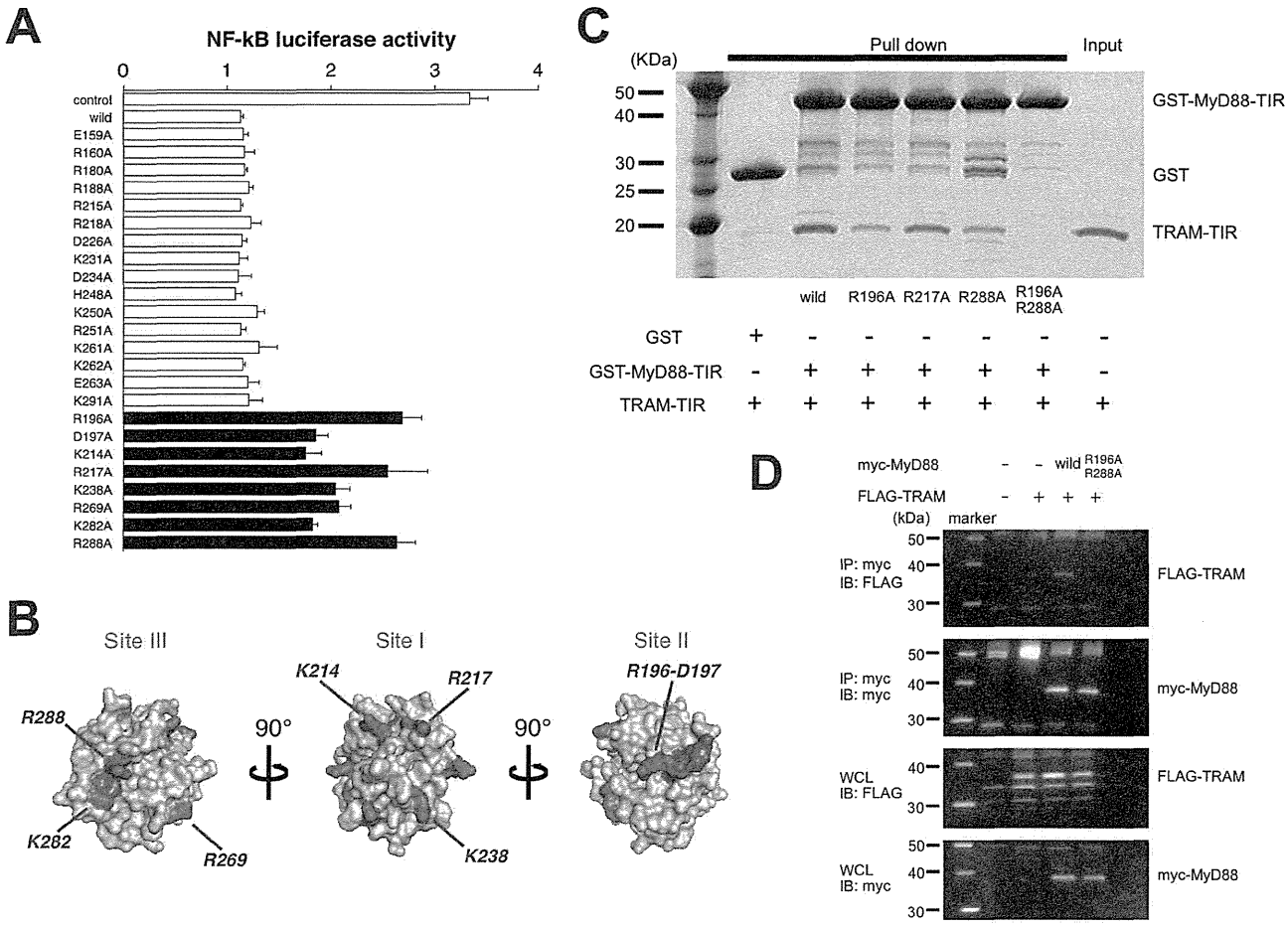

Figure 6. The interaction sites of MyD88 with TRAM. (A) Luciferase reporter gene activities with wild type and mutant types of the MyD88 TIR domain after IL-18 stimulation. The black bars indicate that the residues show significant difference with wild type. (B) The functional assays of IL-18 signaling presented on the 3D structure of the TIR domain of MyD88. Results of the functional assays are mapped onto the molecular surface of the MyD88 TIR domain. The amino acid residues judged to be significant by the luciferase assay are shown in red, while non-significant ones are shown in light brown. The conserved motifs of boxes 1–3 (FDA of box1, VLPG of box2, FW of box3) are shown in blue. (C) Assay to study the binding of the wild type or mutant TRAM TIR domain and MyD88 TIR domain. The representative alanine substitutions at Site II (R196A) or Site III (R288A) in MyD88 caused a reduced interaction with TRAM. The double alanine substituted mutant at Site II and Site III caused the complete abrogation of the interaction with TRAM. (D) Immunoprecipitation assay between MyD88 wild or R196A–R288A mutant, and TRAM.
doi:10.1371/journal.pone.0038423.g006

mutations at both residues leads to a total loss of binding (Figure 6C and 6D). With this dual binding mode via Sites II and III, TRAM would be more efficient at recruiting MyD88 to membrane regions. It should be noted that this dual binding mode was also found in the binding between the MyD88-TIR and Mal-TIR [12], which implies that this sort of multiple binding mode is common to the TIR-containing adaptor proteins.

Additionally, in human, the deficiencies of TIR domain containing adaptors, MyD88 and TRIF, have been recently reported [29,30]. These deficiencies were categorized into the innate immune defects. One of the mutations of MyD88, R196C, is known to cause the severe pyogenic bacteria infection due to the loss of interaction between TLR2, Mal and MyD88 [12]. According to the above-mentioned results, Arg196 is one of the binding sites of MyD88 to TRAM. Therefore, the substitution of Arg196 may abrogate not only an initial signaling of TLR mediated by the interaction between Mal and MyD88 but also a secondary enhancement of immune responses mediated by IL-18 induced interaction between TRAM and MyD88 in T cells or NK cells for etiology of human MyD88 deficiency syndrome.

In summary, we have established an unexpected connection between TRAM and IL-18 signaling, which is mediated by a direct TIR-TIR interaction between MyD88 and TRAM, and we proposed that TRAM is the sorting adaptor for IL-18 signaling. Based on the results obtained in this study, we present a schematic model for signal initiation from activated IL-18 (Figure S2) that is similar to the model for the LPS/TLR4 system.

Materials and Methods

Vector Preparations

The following recombinant protein expression cassettes were subcloned into pGEX4T-1, pGEX5X-1 or pGEX5X-3 (GE Healthcare, Buckinghamshire, England): IL-18, IL-1β, MyD88-TIR (amino acid residues 148–296), TRAM-TIR (66–235), TLR1-TIR (625–786), IL-18Rα-TIR (374–541), and IL-18Rβ-TIR (407–599). A cDNA encoding the MyD88 TIR domain tagged at the N-terminus with a Myc-epitope was cloned into the plasmid vector pcDNA3.1+ (Invitrogen, California, USA). IL-18Rβ and TRAM constructs tagged at the C-terminus with an

AU1- or FLAG-epitope, respectively, were also cloned into pcDNA3.1+. Mutants of TRAM and the TIR domain of MyD88 were generated using the GeneEditor *in vitro* Site-Directed Mutagenesis System (Promega, Wisconsin, USA). A pGL3-Basic Vector (Promega) containing four κB binding sites, which was used in the NF-κB luciferase reporter assay, and a Renilla luciferase reporter vector used as an internal control in the assay were gifts from Dr. Sewon Ki and Dr. Tetsuro Kokubo (Yokohama City University). An IFN-β promoter region sequence containing pGL4-Luc (Promega) was generated. A pAcGFP-C1-MyD88 (GFP-MyD88) and a pDsRed-Monomer-N1-TRAM (DsRed-TRAM) were also generated (Takara Bio, Shiga, Japan).

Protein Expression and GST Pull Down Assay

The TIR domain of the MyD88 wild type and mutants (R196A, R217A, R288A, and R196A–R288A) and the IL-18 receptors (Rα and Rβ) were purified as GST (glutathione S-transferase) fusion proteins according to methods previously described (1). The TIR domain of human TRAM and TLR1 was also obtained by a similar procedure as previously described for the MyD88-TIR. These purified proteins were incubated with Glutathione Sepharose 4B (GE Healthcare) for three hours at 4°C, and then these resins were washed four times with wash buffer (20 mM potassium phosphate buffer (pH 6.0), 100 mM KCl, 0.1 mM EDTA, 10 mM DTT, and 0.5% Triton X100), and then analyzed by SDS polyacrylamide gel electrophoresis with Coomassie Brilliant Blue staining. Experiments were performed in triplicate. The mature form of human IL-18 and IL-1β were prepared using E.Coli expression system according to previously reported methods [15].

Cell Culture

HEK293-hTLR4-MD2-CD14 cells were purchased from Invivogen (California, USA), respectively. HEK293 cells were cultured in Dulbecco's Modified Eagle Medium (high glucose-containing D-MEM, Invitrogen) supplemented with 10% heat-inactivated fetal bovine serum (SIGMA-ALDRICH, Missouri, USA), penicillin (100 U/mL) and streptomycin (100 μg/mL). All cells were incubated at 37°C in a humidified atmosphere of 5% CO2. The splenic pan T cells were isolated using Pan T Cell Isolation Kit II (Miltenyi Biotec, Bergisch Gladbach, Germany) from the spleen of TRAM-deficient mice, MyD88-deficient mice and background mice (C57BL/6) supplied by Oriental Bio Service (Kyoto, Japan). The purified splenic T cells were incubated with or without 2 ng/ml recombinant murine IL-12 (p70) (PEPROTECH, New Jersey, USA) on BIOCOAT anti-mouse CD3 T-cell activation plates (BD Biosciences, Massachusetts, USA) in order to be differentiated into Th1 cells. After 4 days of culture, T cells were washed and restimulated with 20 ng/ml recombinant murine IL-18 (MBL, Nagoya, Japan) and/or 2 ng/ml recombinant murine IL-12 (p70) on anti-mouse CD3 T-cell activation plates for 24 hours. All animal experiments were carried out in accordance with the NIH Guide for Care and Use of Laboratory Animals. These cells were cultured in RPMI1640 media (Invitrogen) supplemented with 10% heat-inactivated fetal bovine serum, penicillin (100 U/mL) and streptomycin (100 μg/mL).

Co-immunoprecipitation Analysis

HEK293T cells in 100 mm plates were transfected with 5.0 μg of pcDNA3.1+ IL-18Rβ, 5.0 μg of pcDNA3.1+ Myc-tagged MyD88 (full-length) wild or R196A–R288A mutant and/or 5.0 μg of pcDNA3.1+ FLAG-tagged TRAM (full-length) using Lipofectamine 2000 (Invitrogen). After 18 hours, the culture media were replaced. After 24 more hours, the cells were incubated with or without IL-18 (10 ng/mL). These cells were washed with cold PBS and harvested with cell lysis buffer (Tris-HCl buffer (pH 7.5) with 10 mM NaCl, 10 mM EDTA, 0.5% Triton-X100, a protease inhibitor cocktail (Roche Diagnostics, Mannheim, Germany), and a phosphatase inhibitor cocktail (PIERCE, Illinois, USA). The soluble cell lysates including 1000 μg protein were incubated with 5 μg of anti-Myc antibody (Invitrogen) or anti-FLAG M2 monoclonal antibody (SIGMA-ALDRICH) for 60 minutes; 50 μl of MultiMACS Protein G MicroBeads (Miltenyi Biotec) that had been equilibrated with cell lysis buffer for 30 minutes at 4°C was then added to the lysates. After incubation, the immune complexes were applied to the magnetic columns. The protein complex samples were then solubilized with 1× Laemmli sample buffer after four washes with wash buffer. The samples were analyzed by western blots using an anti-Myc antibody and an anti-FLAG M2 monoclonal antibody.

Knock-down with shRNA or Dominant Negative Mutant of TRAM

The shRNA expression vector psiRNA-h7SKgz-Scr (used as a negative control because it contained a scrambled sequence) and psiRNA-TICAM-2 were purchased from Invivogen. For the reporter gene assays, HEK293T or HEK293-hTLR4-MD2-CD14 cells were seeded at a density of 2.0×10^5 cells/mL per well in a 96-well plate. These cells were transfected with or without pcDNA3.1+ IL-18Rβ-AU1, NF-κB luciferase reporter vector, and Renilla luciferase reporter vector with either the psiRNA-h7SKgz-Scr or psiRNA-TICAM-2, pcDNA3.1+ TRAM-FLAG wild or C117H mutant vector using Lipofectamine 2000. After 18 hours, the culture media were replaced with fresh medium, and after an additional 24-hour incubation, the culture media were replaced with fresh medium containing recombinant human IL-18 (2.0, 5.0, 50.0 or 10.0 ng/mL) or LPSO127: B8, which is derived from *E. Coli* strain (100 ng/mL) (SIGMA-ALDRICH), incubated for 6 hours. The luciferase reporter gene activities were analyzed using a Dual-Luciferase Reporter Assay System (Promega). The statistical significance of the differences in the luciferase activities was determined using Dunnett's multiple comparison test. The statistical significance was assigned to be $P<0.05$.

RT-PCR

Total RNA from cells seeded in six-well plates was isolated with ISOGEN (Nippon Gene, Toyama, Japan) according to the manufacturer's instructions. Reverse transcription was performed with a 1st Strand cDNA Synthesis Kit (Roche Diagnostics) according to the manufacturer's instructions. The cDNA obtained was used in PCR with Taq DNA polymerase (Toyobo, Osaka, Japan) to determine the relative amount of TRAM mRNA.

ELISA

Culture supernatants in test tubes were centrifuged to remove the cells and then stored at −80°C until analysis. The IFN-γ concentrations were measured using a Mouse IFN-γ Quantikine ELISA Kit (R&D Systems, Minnesota, USA). The statistical significance of the differences in the cytokine productions between the wild type cells and the TRAM or MyD88 deficient cells was determined using two-way ANOVA with Bonferroni's multiple comparison test. The statistical significance was assigned to be $P<0.05$.

Confocal Microscopy

For direct immunofluorescence, HEK293T cells co-transfected GFP-MyD88 and DsRed-TRAM were washed in phosphate-